



## 저작자표시-비영리-변경금지 2.0 대한민국

이용자는 아래의 조건을 따르는 경우에 한하여 자유롭게

- 이 저작물을 복제, 배포, 전송, 전시, 공연 및 방송할 수 있습니다.

다음과 같은 조건을 따라야 합니다:



저작자표시. 귀하는 원저작자를 표시하여야 합니다.



비영리. 귀하는 이 저작물을 영리 목적으로 이용할 수 없습니다.



변경금지. 귀하는 이 저작물을 개작, 변형 또는 가공할 수 없습니다.

- 귀하는, 이 저작물의 재이용이나 배포의 경우, 이 저작물에 적용된 이용허락조건을 명확하게 나타내어야 합니다.
- 저작권자로부터 별도의 허가를 받으면 이러한 조건들은 적용되지 않습니다.

저작권법에 따른 이용자의 권리는 위의 내용에 의하여 영향을 받지 않습니다.

이것은 [이용허락규약\(Legal Code\)](#)을 이해하기 쉽게 요약한 것입니다.

[Disclaimer](#)

보건학 박사학위논문

**Prenatal exposure to bisphenol S and  
influence on obesity in F1 generation**

비스페놀 S 의 산전 노출과 비만 감수성의 변화

2020 년 8 월

서울대학교 보건대학원

환경보건학과 환경보건학 전공

안 영 아

## **Abstract**

# **Prenatal exposure to bisphenol S and influence on obesity in F1 generation**

Yeong-A An

Environmental Health Sciences Major

Graduate School of Public Health

Seoul National University

Bisphenol S (BPS) is increasingly used as a replacement for Bisphenol A (BPA), a known endocrine disruptor. It has been well documented that prenatal exposure to BPA affects not only fetal development but also metabolic diseases including obesity in adolescence and adulthood. While an increasing number of studies has explored whether the structurally similar BPS could likewise affect health outcomes, research on the link between fetal exposure to BPS and adiposity in later life is still underexplored.

The overall goal of this study is to investigate the adiposity effects of prenatal exposure to BPS in adult mice. There are three knowledge gaps that need

to be addressed for a better understanding of the effects of early life exposure to BPS on adiposity in later life: (1) whether maternally delivered BPS to the fetus/neonate would be totally transformed to its conjugates and easily excreted is limited; (2) unclear periods of BPS exposure that are linked with adiposity in adulthood; (3) limited evidence of *in vivo* studies on BPS-induced adiposity and epigenetic modification. To address these important knowledge gaps, this study consists of three key studies that make up the main chapters of this dissertation.

In the first study (Chapter 2), each of the BPS metabolites was determined at postnatal day 1 (PND1) to investigate whether maternally delivered BPS was totally excreted and transformed to inactive metabolites such as BPS-glucuronide (BPS-G) and BPS-sulfate (BPS-S). The key hypothesis in Chapter 2 was that maternally delivered BPS may not be totally excreted after birth. Maternal BPS transferred to fetus, and the type of abundant metabolites is different from adult's one. The liver of fetus is not fully developed yet, and thus, it is suspected that it cannot produce BPS-glucuronide at high enough levels to be detected in neonatal livers. Detectable levels of BPS metabolites were available in the tissues in BPS 50 mg/kg/d group. Predominant metabolites of BPS were BPS-S in liver tissues at PND1, and BPS-G in the rest of body in BPS 50 mg/kg/d group. It was found that in a day after the end of perinatal exposure to BPS, the fetal body retained approximately 14.6% of maternally delivered BPS.

The second study (Chapter 3) aimed to investigate the adiposity effects of prenatal exposure to BPS in adult mice. Pregnant mice were exposed to BPS via the drinking water from gestation day 9 until delivery. Then, two groups of offspring (six weeks old) were either fed a standard diet (STD) or high fat diet (HFD) until sacrifice. HFD was fed for 4 weeks. To observe adiposity phenotypes in adult offspring, the body weight and gonadal fat pad mass were measured. To assess changes in adipogenic marker genes, mRNA expression of *Pparg*, *Cebpa*, *Fabp4*, *Lpl* and *Adipoq* was analyzed in gonadal white adipose tissues (gWAT) of all males exposed to BPS. Prenatally BPS-exposed male on a HFD gained body weight and gonadal fat pad mass more than naïve control on the same diet. There were significant increases of mRNA of all adipogenic markers in male BPS-exposed mice fed with HFD. Noticeably, *Lpl* was observed as the BPS-effect in STD-fed males. These findings indicated that prenatal exposure to BPS associated with the upregulation of mRNA expression of the key adipogenic marker genes resulting in the manifestation of adiposity phenotype. Furthermore, we suggest that the elevated *Lpl* mRNA level might be a potential susceptibility marker of BPS-induced adiposity in male offspring.

In the final study (Chapter 4), DNA methylation of adiposity-related imprinting gene in adipose tissue (especially gWAT) was evaluated to explain

whether prenatal exposure to BPS affects fetal reprogramming. *Igf2/H19* was selected as the adiposity-related imprinting gene. The effect of BPS exposure during fetal development on the imprinting gene was investigated with DNA methylation of *Igf2/H19* ICR in gWAT. BPS-related CpG sites of *Igf2/H19* ICR were observed in gWAT. These result suggested that BPS exposure during mid-gestation can alter the levels of DNA methylation in *Igf2* and has an impact of specific CpG sites on it.

Through a series of studies, it was clearly demonstrated that (1) maternally exposure to BPS transferred to fetuses and retained in neonate, (2) prenatal BPS was related to the susceptibility to adiposity in adulthood and (3) altered the levels of DNA methylation in adiposity-related imprinting gene, *Igf2*, in white adipose tissues, and (4) mid-gestation can be a sensitive window of fetal exposure to BPS.

Our findings have important implications for the understanding of the vulnerable period of BPS exposure to the adult-onset obesity in epidemiology. On the context of DOHaD, additional research is needed on expression of adiposity-related imprinting gene resulting from such an exposure to BPS.

**Keywords:** BPS, prenatal exposure, adiposity, adipogenic markers, imprinting gene, DNA methylation

**Student Number: 2016-30659**

# Contents

<b>Chapter 1. Background .....</b>	<b>1</b>
<b>1.1. The emergence of BPS as a replacement for BPA .....</b>	<b>1</b>
1.1.1. Increasing awareness about the health effects of BPA ....	1
1.1.2. The emergence of BPS .....	2
<b>1.2. Human exposure to BPS and its health effects .....</b>	<b>4</b>
<b>1.3. Suggestive vulnerable periods of BPS exposure .....</b>	<b>5</b>
1.3.1. Immature BPS metabolism in fetus .....	5
1.3.2. Susceptible windows of fetal programming .....	8
<b>1.4. The role of EDCs on obesity .....</b>	<b>11</b>
1.4.1. Obesogenic EDCs .....	11
1.4.2. Potential mechanism of obesogenic EDCs .....	12
1.4.3. PPAR $\gamma$ as obesogens target.....	13
1.4.4. Igf2/H19.....	14
<b>1.5. Study design and objectives .....</b>	<b>15</b>
<b>Chapter 2. Delivery of BPS during fetal stage F1.....</b>	<b>19</b>
<b>2.1. Introduction .....</b>	<b>19</b>
<b>2.2. Materials and methods.....</b>	<b>22</b>
2.2.1. Chemicals and reagents .....	22

2.2.2. Animal treatment .....	23
2.2.3. Sample collection and preparation.....	25
2.2.4. Instrument analysis .....	27
2.2.5. Quality assurance (QA) and quality control (QC).....	32
2.2.6. Calculation of $\sum$ BPS metabolites .....	34
<b>2.3. Results.....</b>	<b>35</b>
2.3.1. Determination of BPS metabolites at PND 1 .....	35
2.3.2. Sum of BPS metabolites remained at PND 1 .....	36
<b>2.4. Discussion .....</b>	<b>39</b>

## **Chapter 3. Adipogenic effects of prenatal exposure to BPS in adult F1 male mice.....42**

<b>3.1. Introduction .....</b>	<b>42</b>
<b>3.2. Materials and methods.....</b>	<b>46</b>
3.2.1. Animal treatment .....	46
3.2.2. Measurement of the body weight and fat pad mass of the offspring.....	50
3.2.3. Measurement of food intake and energy expenditure....	51
3.2.4. Histological analysis of the gWAT .....	52
3.2.5. Reverse- transcription quantitative PCR analysis.....	53
3.2.6. Statistical analysis.....	55
<b>3.3. Results.....</b>	<b>56</b>



3.3.1. Body weight and fat mass.....	56
3.3.2. Food intake and energy expenditure.....	60
3.3.3. Adipocyte hypertrophy in the gWAT .....	62
3.3.4. mRNA expression of adipogenic marker genes.....	65
<b>3.4. Discussion .....</b>	<b>68</b>
3.4.1. Body weight and gWAT changes after prenatal exposure to BPS under HFD-challenge at adult F1 mice .....	68
3.4.2. Upregulation of adipogenesis-related transcription in the gWAT .....	72
<b>Chapter 4. BPS-responsive DNA methylation of <i>Igf2</i> in adult F1 male mice .....</b>	<b>79</b>
<b>4.1. Introduction .....</b>	<b>79</b>
<b>4.2. Materials and methods.....</b>	<b>82</b>
4.2.1. DNA isolation and bisulfite conversion.....	82
4.2.2. PCR amplifications and Pyrosequencing analysis.....	83
4.2.3. Statistical Analysis.....	85
<b>4.3. Results.....</b>	<b>86</b>
4.3.1. DNA methylation of <i>H19/Igf2</i> ICR in gWAT .....	86
4.3.2. BPS-related CpG sites on <i>Igf2/H19</i> in gWAT.....	88
<b>4.4. Discussion .....</b>	<b>93</b>

<b>Chapter 5. Overall conclusions.....</b>	<b>97</b>
<b>Bibliography.....</b>	<b>102</b>
<b>국 문 초 록 (Abstract in Korean).....</b>	<b>121</b>

## List of Tables

Table 2-1. Instrument condition.....	29
Table 2-2 Accurate m/z ratio of the [M-H] <sup>-</sup> precursor ions, total fragment ions found by MS/MS.....	31
Table 2-3. Calibration curve and the regression coefficient ( $R^2$ ).....	33
Table 2-4. LOD, LLOQ and ULOQ in liver at PND1 .....	33
Table 2-5. LOD, LLOQ and ULOQ in the rest of body at PND1.....	33
Table 2-6. Concentration and detection rates of BPS metabolites at PND1 (n=5) 37	
Table 2-7. The sum of amount of BPS metabolites at PND 1 (n=5) .....	38
Table 3-1. Applied doses of bisphenol S adjusted to the maternal body weight ...	48
Table 3-2. The number of dams and male offspring in the bisphenol S exposure group .....	49
Table 3-3. Primers for quantitative reverse-transcription PCR analysis.....	54
Table 3-4. Coefficient of variations for body weight and the relative mass of gonadal white adipose tissue to the body weight .....	69

## List of Figures

Figure 1-1. Bisphenols structure: (a) Bisphenol A, (b) Bisphenol S. ....	3
Figure 1-2. Proposed metabolism of bisphenol S in rodents (SULTs, sulfo- transferases; UGTs, uridine 5'-diphosphoglucuronosyl-transferases; CYP, cytochrome P450). Waidyanatha et al. (2018).....	6
Figure 1-3. Plasticity of cell differentiation (Ost and Pospisilik 2015). ....	9
Figure 1-4. <i>Igf2/H19</i> domain (Susiarjo et al. 2013).....	14
Figure 1-5. Overview of the study design and dissertation .....	17
Figure 1-6. Overview of animal experiment design. ....	18
Figure 2-1. Chromatogram of BPS metabolites in the rest of body of PND1. ....	30
Figure 3-1. Schematic representation of the experimental protocol. BPS, bisphenol S; STD, standard diet; HFD, high-fat diet; GD, gestational day. ....	49
Figure 3-2. Effects of prenatal exposure to bisphenol S on body weight and the ratio of gonadal white adipose tissue (gWAT) to body weight in F1 male mice administered a standard diet (STD) or a high-fat diet (HFD). (a) Body weight in offspring administered an STD (left) and an HFD (Braun et al.), (b) The ratio of gWAT mass to body weight in offspring administered an STD (left) and an HFD (Braun et al.). Values represent the mean $\pm$ SD for each group. The least-squares (LS) means of the phenotypes significantly increased from	

5 mg/kg/d ( $p = 0.0036$ for BW, $p = 0.0018$ for gWAT/BW) in the HFD group, as revealed through the <i>a priori</i> contrast test. LS-means with the same letter are not significantly different. No letters in the subpanel imply the absence of treatment effects of BPS. ....	57
Figure 3-3. The ratios of fat mass to body weight (%) of the offspring ( $n = 15$ ) administered a high-fat diet. Values represent the mean $\pm$ SD for each group. ....	59
Figure 3-4. Food intake and energy expenditure among offspring ( $n = 15$ ) administered a high-fat diet. (a) Food intake during the day and night in three male mice by group, (b) energy expenditure (EE) in six male mice by group. Representative data on EE were normalized to the metabolic mass (lean mass + 0.2 fat mass) (Even and Nadkarni 2012). LS-means with the same letter are not significantly different on an <i>a priori</i> contrast test. Values represent the mean $\pm$ SD for each group. No letters in the subpanel implies the absence of treatment effects of bisphenol S.....	61
Figure 3-5. Effect of prenatal exposure to bisphenol S (BPS) on adipocyte hypertrophy in the gonadal white adipose tissue (gWAT) in F1 male mice administered a high-fat diet (HFD). (a) Representative images (magnification, 100 $\times$ ) of hematoxylin-eosin-stained gWAT sections of 3 mice per exposure group, 3 sections per mouse, and 3 fields per section, (b) Adipocyte area from gWATs in each group ( $n = 45$ ), (c) Adipocyte diameter from gWATs in each	

group ( $n = 45$ ). Values represent the mean $\pm$ SD for each group.....	63
Figure 3-6. Least-squares (LS) means of relative mRNA expression of <i>Pparg</i> and its direct target genes in the gonadal white adipose tissue (gWAT) in F1 male mice prenatally-exposed to bisphenol S and those exposed to the vehicle control. STD - standard diet, HFD - high-fat diet. Each value represents the fold-change of relative mRNA expression levels to the average of each vehicle group (mean $\pm$ SD). mRNA upregulation was prominent from 5 mg/kg/d [ <i>Pparg</i> ( $p = 0.0010$ ), <i>Lpl</i> ( $p = 0.005$ ) and <i>Adipoq</i> ( $p = 0.0039$ )] and 50 mg/kg/d [ <i>Cebpa</i> ( $p = 0.0001$ ) and <i>Fabp4</i> ( $p = 0.0002$ )] on <i>a priori</i> contrast tests. LS-means with the same letter are not significantly different. No letters in the subpanel imply the absence of the effects of BPS. ....	67
Figure 4-1. The overall level of DNA methylation on <i>Igf2/H19</i> ICR in gonadal adipose tissues of F1 male mice prenatally exposed to BPS. STD; standard diet, HFD; high-fat diet.....	87
Figure 4-2. The levels of DNA methylation at six CpG sites on <i>Igf2/H19</i> ICR in gonadal adipose tissues of F1 male mice prenatally exposed to BPS. (a) DNA methylation at CpG1 on <i>Igf2/H19</i> ICR. (b) DNA methylation at CpG2 on <i>Igf2/H19</i> ICR. (c) DNA methylation at CpG3 on <i>Igf2/H19</i> ICR. (d) DNA methylation at CpG4 on <i>Igf2/H19</i> ICR. (e) DNA methylation at CpG5 on <i>Igf2/H19</i> ICR. (f) DNA methylation at CpG6 on <i>Igf2/H19</i> ICR. The black diamonds in the boxplots represent the mean values and the grey dots represent	

the individual sample data. ....	92
----------------------------------	----

# Chapter 1. Background

## 1.1. The emergence of BPS as a replacement for BPA

### 1.1.1. Increasing awareness about the health effects of BPA

BPA is a chemical compound used in the manufacture of polycarbonate plastics and epoxy resins that are pervasive in daily life. According to occupational exposure studies, workers who manufacture products that contain BPA were exposed (Hines et al. 2017). Exposure, however, is not limited to people involved in the manufacturing process. For example, cashiers undergo dermal exposure when handling thermal paper receipts containing BPA on a daily basis (Hehn 2016; Porras et al. 2014). In the general population, human exposure to BPA mainly comes from eating food or drinking water stored in containers made from plastic (Christensen et al. 2012; Lorber et al. 2015; Matsumoto et al. 2003), as the BPA can leach into the stored food. Besides the general population (Lakind and Naiman 2008), especially the exposure of pregnant women, infant, and children to BPA has been discussed in prior literature (Callan et al. 2013; Mendonca et al. 2014; Zhang et al. 2013).

BPA is known as an endocrine disruptor and increased levels of BPA in adults have been correlated with various diseases. The vulnerability of early life



staged-population (infants and children) to the adverse effects of BPA has also been well established. This has resulted in the use of BPA in baby bottles being prohibited in Canada, the European Union, and the United States. BPA has also been prohibited from being used in food contact materials that are targeting contact with children in France, Denmark and Belgium (EU 2011). It's use in baby-soothers and cash receipts has been banned in Austria and Sweden, respectively (EU 2011). The USFDA has amended its regulations to no longer provide for the use of BPA-based baby bottles and sippy cups in 2012 (USFDA 2012), and infant formula packaging in 2013 (USFDA 2013). In addition, South Korea's Ministry of Food and Drug Safety (MFDS) implemented a plan to ban BPA in food contact materials for infants and young children that will come into effect in 2020.

#### **1.1.2. The emergence of BPS**

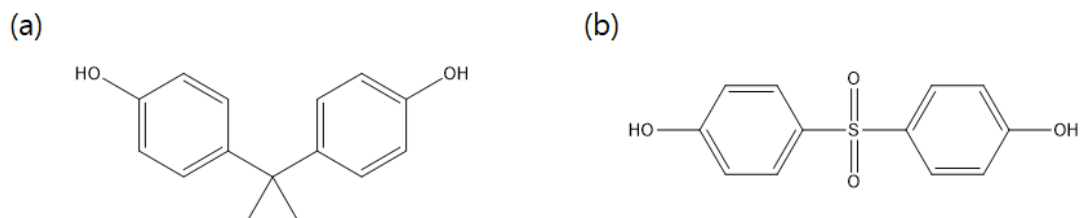
Since the negative effects of BPA, a representative endocrine disrupting chemicals (EDCs), have been verified in animal models (e.g., Fang et al. 2015; Vandenberg et al. 2013; Wei et al. 2011) and human epidemiology (WHO/FAO 2011), the public discussion about these results has resulted in a noticeable trend towards "BPA-free" offerings in many product categories.

BPA is increasingly replaced by BPS, a structurally similar compound having two phenol groups (see Figure 1-1) Production volume of BPS in the U.S. amounted to between 0.5 and 5 million tons in 2012 (U.S. EPA 2010a, 2010b).

According to ECHA (<https://echa.europa.eu/-/bpa-being-replaced-by-bps-in-thermal-paper-echa-survey-finds>), the market-share of BPS-based thermal papers is expected to continue to increase in the coming years, in particular after a ban on the use of BPA in thermal paper in the EU will come into effect in January of 2020.

With an increased usage of BPS in a wide range of countries (Chen et al. 2016), occurrence of BPS has been reported in various environment matrices (Eckardt and Simat 2017; Liao and Kannan 2013, 2014; Liu et al. 2018; Yan et al. 2017). In fact, it has already surpassed BPA in certain areas (Asimakopoulos et al. 2016; Liao et al. 2012).

Figure 1-1. Bisphenols structure: (a) Bisphenol A, (b) Bisphenol S.



## **1.2. Human exposure to BPS and its health effects**

The widespread adoption of BPS is indicated by the fact that BPS has been detected in over 80% of human urine samples in the US (Lehmle et al. 2018) and Saudi Arabia (Asimakopoulou et al. 2016). Urinary BPS was also detected in pregnant women from Canada (J Liu et al. 2017; Liu et al. 2018) and China (Wan et al. 2018), which might imply that maternal exposure to BPS can reach fetal circulation by crossing the placenta (J Liu et al. 2017). Importantly, according to cross-sectional studies, a higher BPS concentration was observed in obese rather than non-obese US adults (B Liu et al. 2017; Liu et al. 2019).

Despite widespread use of BPS and human exposure, less is known about toxicity of BPS. Initial studies have indicated that BPS may cause toxic effects that are similar to BPA (Rochester and Bolden, 2015, Auerbach et al., 2016). ECHA's Risk Assessment Committee indicated that BPS "is suspected to have many of the same adverse health effects as BPA".

However, many toxicity of BPS were comparable to those of BPA (Ahmed and Atlas 2016; Boucher et al. 2016b; Helies-Toussaint et al. 2014; Silva et al. 2019; Vinas and Watson 2013; Zhang et al. 2018). Considering emerging toxic effect of BPS, questions about the safety of BPS have become an important issue (Rochester and Bolden 2015).

### **1.3. Suggestive vulnerable periods of BPS exposure**

#### **1.3.1. Immature BPS metabolism in fetus**

It is well-known that xenobiotic chemicals are metabolized by phase I and II. Information on these metabolism has been generated with fully functional hepatocyte, adult animal and human. Recent study reported that the liver is a main site of BPS metabolism, and the intestine is additional site that BPS can be metabolized (Skledar et al. 2016). For fetus and neonate, the liver and GI tract are immature and continues developing after birth until it reaches its mature size. Thus, BPS cannot be fully metabolized and excreted during fetal development, when that is transferred to the developing fetus through the maternal placenta during pregnancy (Gingrich et al. 2018; Wan et al. 2018).

BPS can firstly undergo metabolic activation in the presence of microsomes, the major source of oxidative enzymes including cytochromes P450 (CYPs). In this phase I biotransformation (oxidation), BPS is hydroxylated. BPS metabolized to BPS-glucuronide (BPS-G) and BPS-sulfate (BPS-S) in phase II biotransformation (conjugation). The enzymes of phase II, uridine diphosphoglucuronosyltransferases (UGTs), are distributed in many tissues including liver and intestine. UGT1A9, an isoform that is found predominantly in liver, is the most active with BPS as substrate (Waidyanatha et al. 2018).

Pathway of BPS metabolism by metabolic enzymes is depicted in

Waidyanatha et al. (2018).

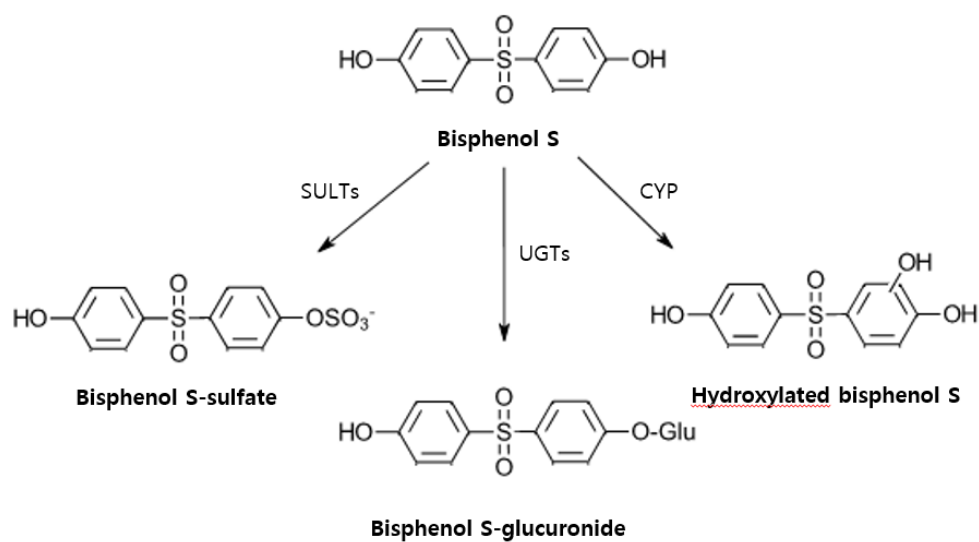


Figure 1-2. Proposed metabolism of bisphenol S in rodents (SULTs, sulfo-transferases; UGTs, uridine 5'-diphosphoglucuronosyl-transferases; CYP, cytochrome P450).

Waidyanatha et al. (2018).

In adult sheep, the metabolite excreted in urine is BPS-G, whereas BPS-S and free BPS are dominant in feces (Grandin et al. 2017). Indeed, BPS-G is mainly produced as 97% of the BPS in human urine was detected as the conjugated form (Zhou et al. 2014). However, the metabolism and excretion are different in fetal ovine. In the ovine model, fetal BPS-G remained trapped and underwent its back-conversion into bioactive BPS, i.e., free BPS, once maternally delivered BPS was metabolized into BPS-G (Grandin et al. 2018). Information on fetal metabolism and internal dose of BPS is essential to understand the adverse health effect in later life as free BPS and hydroxylated BPS play important roles in terms of toxicity. According to previous studies, BPS-G, unlike free-BPS and hydroxylated BPS (HO-BPS), did not bind to estrogen and thyroid receptors (Skledar et al. 2016). BPS-S did not show hER $\alpha$  (humanized estrogen receptor alpha) activity when HepG2 and MELN cells were used (Le Fol et al. 2015).

It is important to investigate whether active formed BPS metabolite is retained in the fetal body in that BPS can bind and activate nuclear receptors such as ERs (estrogen receptors) and ERRs (estrogen related receptors). Nevertheless, not only are the predominant fetal metabolites of BPS yet unknown, also in vivo studies on the fetal internal dose of BPS following maternal exposure to BPS have been limited to date.

### 1.3.2. Susceptible windows of fetal programming

Based on the Developmental Origins of Health and Disease (DOHaD) concept, studies on obesity often focus on *in utero* exposure (e.g., Barrett 2017; Breton et al. 2017; Yamada and Chong 2017). The ‘fetal origins’ hypothesis has supported that environment exposure in early life can contribute to metabolic and cardiovascular diseases in later life (Armitage et al. 2008). Although existing human data on BPA and metabolic diseases are limited, prenatal exposure to BPA has been linked to the development of metabolic diseases such as obesity and diabetes in adult offspring (Alonso-Magdalena et al. 2010; Vom Saal et al. 2012; Wassenaar et al. 2017). It is noted that the DOHaD hypothesis describes that the developmental plasticity regulating adaptation to environmental challenges is determined in the process of epigenetic programming.

In the context of adipogenesis, many *in vitro* studies have shown EDC-induced epigenetic effect using preadipocyte differentiation model. Adipocyte programming appear to link to sensitive periods for environmental input in the differentiation process (Figure 1-3). Given the plasticity of adipocyte differentiation during fetal programming, prenatal BPS-induced adipogenic effect should be investigated linking to epigenetic alteration.

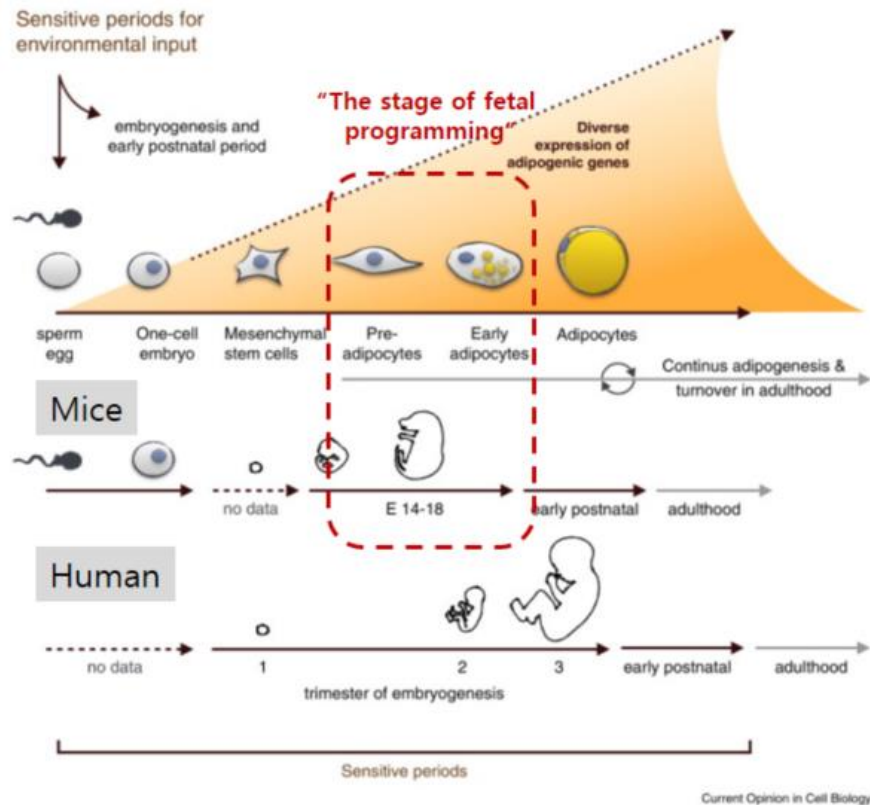


Figure 1-3. Plasticity of cell differentiation (Ost and Pospisilik 2015).

The traditional view of cell differentiation pictures cell differentiation as a linear event leading to a predestined uniform cell population. Intergenerational/transgenerational inheritance of environmental states and epigenetic modulation of tissue generation now suggests that there is a substantial plasticity in these processes. In Figure 1-3, this is illustrated for adipocyte development. The variation within a lineage specification is set by parental, embryonic and early life cues and the sensitive periods correlate with vital stages



in the process in cell differentiation (Ost and Pospisilik 2015).

In another perspective, imprinted genes are thought to determine early life EDCs-induced adiposity (Drobna et al. 2018; Susiarjo et al. 2013). During early embryogenesis, several major global epigenetic alterations occur in the genome that regulate the timely expression or repression of development-associated genes (Reik 2007). Parental epigenetic marks are first removed after fertilization, which allows for reprogramming of the marks, partly under the influence of environmental triggers (Reik 2007). However, parentally imprinted genes are not removed during this period (Perera and Herbstman 2011). IGF-2, one of imprinted genes, has been the most studied. According to the Dutch Hunger Winter study, altered imprinting of IGF-2 is correlated with higher fat deposition. Exposure to BPA during early development has been found to induce similar responses.

## **1.4. The role of EDCs on obesity**

### **1.4.1. Obesogenic EDCs**

The focus of EDC research has long been placed on estrogens, androgens and thyroid agonists and antagonists, but it is now clear that there are EDCs that affect other receptors and metabolic systems (Schug et al. 2011).

It is no doubt that the main factors promoting obesity are a disruption of the body energy balance and genetic background. However, this does not fully explain the increased prevalence of obesity in the last several decades. It has been noted that, concurrently with the increase in obesity, human exposure to synthetic chemicals has increased (Baillie-Hamilton 2002). The term “environmental obesogens” was first used for organotins possessing obesogenic properties which can disrupt the normal developmental and homeostatic controls over adipogenesis and energy balance (Grun and Blumberg 2006). Exposure to obesogenic EDCs, as a subset of environmental factors, experienced during fetal development have significant impacts on obesity susceptibility later in life.

Recent reviews of literature have summarized that obesogenic EDCs may contribute to regulating and promoting lipid accumulation and adipogenesis, especially if exposure occurs at an early life stage (Darbre 2017; Heindel et al. 2015; Veiga-Lopez et al. 2018).

#### **1.4.2. Potential mechanism of obesogenic EDCs**

Adverse intrauterine events have been associated with subsequent obesity and metabolic disease in so-called “fetal programming” (Barker et al. 1993), but the underlying mechanisms for this are not well understood.

The proposed mechanism by which early life EDC exposure can affect epigenetic programming of obesity has been reviewed by (Heindel et al. 2015). EDCs are structurally similar to many hormones, and are thus capable of mimicking natural hormones and maintain similar modes of action, transport, and storage within tissues. These characteristics results in EDCs being well suited to activate or antagonize nuclear hormone receptors (Diamanti-Kandarakis et al. 2009).

#### 1.4.3. PPAR $\gamma$ as obesogens target

White adipose tissue metabolism is under the control of the sympathetic nervous system and is modulated by hormones including sex steroids. The impact of environmental estrogens on adipose tissue may be through direct modulation of lipogenesis, lipolysis, and adipogenesis (Cooke and Naaz 2004).

Mature adipocytes are generated from multipotent stromal cells (MSCs) found in almost all fetal and adult tissues. MSCs can differentiate into bone, adipose tissue, cartilage, muscle, *in vitro* and are thought to help maintain these tissues in the adult. *In vitro* experiments have demonstrated that EDCs promote changes in mesenchymal stem cells (MSCs), leading to increases in adipogenic differentiation.

PPAR $\gamma$  is thought to be the master regulator of adipogenesis because it plays an important role in nearly all aspects of adipocyte biology (Evans et al. 2004). Activation of PPAR $\gamma$ 2 in pre-adipocytes induces them to differentiate into adipocytes and PPAR $\gamma$  is required for this process *in vitro* and *in vivo* (Rosen et al. 1999). It is known that humans whose diabetes is being treated with rosiglitazone (a drug that activates PPAR $\gamma$ ) develop more adipocytes and gain weight (Shim et al. 2006).

Therefore, it is reasonable to hypothesize that BPS capable of activating PPAR $\gamma$  might have the same effect because adipogenesis is continuous during fetal development (Figure 1-3).

#### 1.4.4. *Igf2/H19*

The use of *Igf2/H19*, which is related to adiposity, is suitable as differential DNA methylation is a well-characterized imprinting mechanism. And, that is developmentally critical as it is essential for embryonic, placenta and postnatal growth. A clinical research reported that the ICR of the IGF2/H19 locus was associated with greater adiposity in young adults (Huang et al. 2012). BPA disrupted proper expression of imprinted genes in a gene- and tissue-specific manner when exposure occurs early in development.

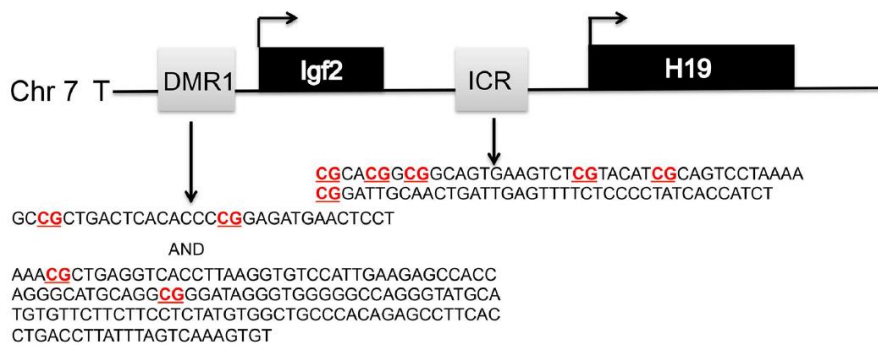


Figure 1-4. *Igf2/H19* domain (Susiarjo et al. 2013).

## **1.5. Study design and objectives**

The overall goal of this study is to investigate the adiposity effects of prenatal exposure to BPS in adult mice. There are three knowledge gaps that need to be addressed in order to gain a better understanding of the effects of early life exposure to BPS on adiposity in later life: (1) information on whether maternally delivered BPS to the fetus would be totally transformed to inactive conjugate form is limited (2) critical periods of BPS exposure that are linked with adiposity in adulthood are yet unclear; (3) existing *in vivo* studies on BPS-induced adiposity are still limited. To address these important knowledge gaps, this study consists of four key studies that make up the main chapters of this dissertation.

In the first study (Chapter 2), each of the BPS metabolites was determined at postnatal day 1 (PND1) to investigate whether maternally delivered BPS was totally excreted and transformed to inactive metabolites such as BPS-G and BPS-S. The key hypothesis addressed in Chapter 2 was that maternally delivered BPS may not be totally excreted after birth.

In the second study (Chapter 3), fetal BPS-induced changes in adiposity phenotypes were investigated in adult-staged offspring. In order to stimulate adiposity development, mice were fed a HFD for four weeks. Body weight and fat mass were measured as indicators for adiposity. The adipocyte number and size

were also assayed in gonadal white adipose tissue of male offspring. Furthermore, mRNA expression of adipogenic marker genes in gonadal white adipose tissue was analyzed to elucidate the regulation of adipogenesis.

In the final study (Chapter 4), DNA methylation of adiposity-related imprinting gene in adipose tissue (especially gWAT) was evaluated to explain whether prenatal exposure to BPS affects fetal reprogramming. *Igf2/H19* was selected as the adiposity-related imprinting gene. We investigated effects of exposure on genomic imprinting in the mouse as imprinted genes are regulated by differential DNA methylation and aberrant imprinting disrupts fetal, placental, and postnatal development.

The results from these four studies allow to better understand the effect of early life exposure to BPS on adiposity in later life by investigating the alteration of adult adiposity susceptibility and by establishing a link between fetal reprogramming and adiposity.

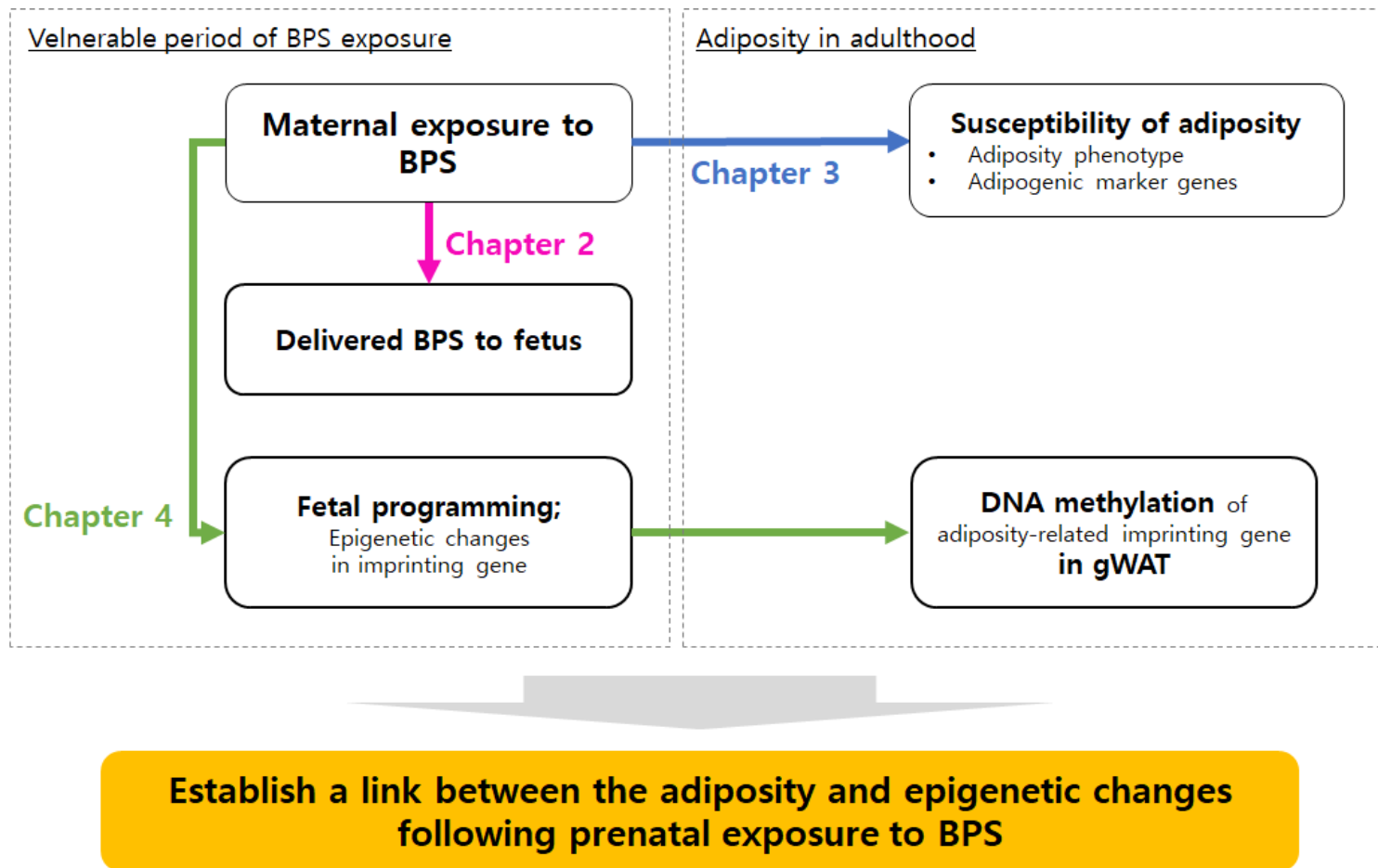


Figure 1-5. Overview of the study design and dissertation



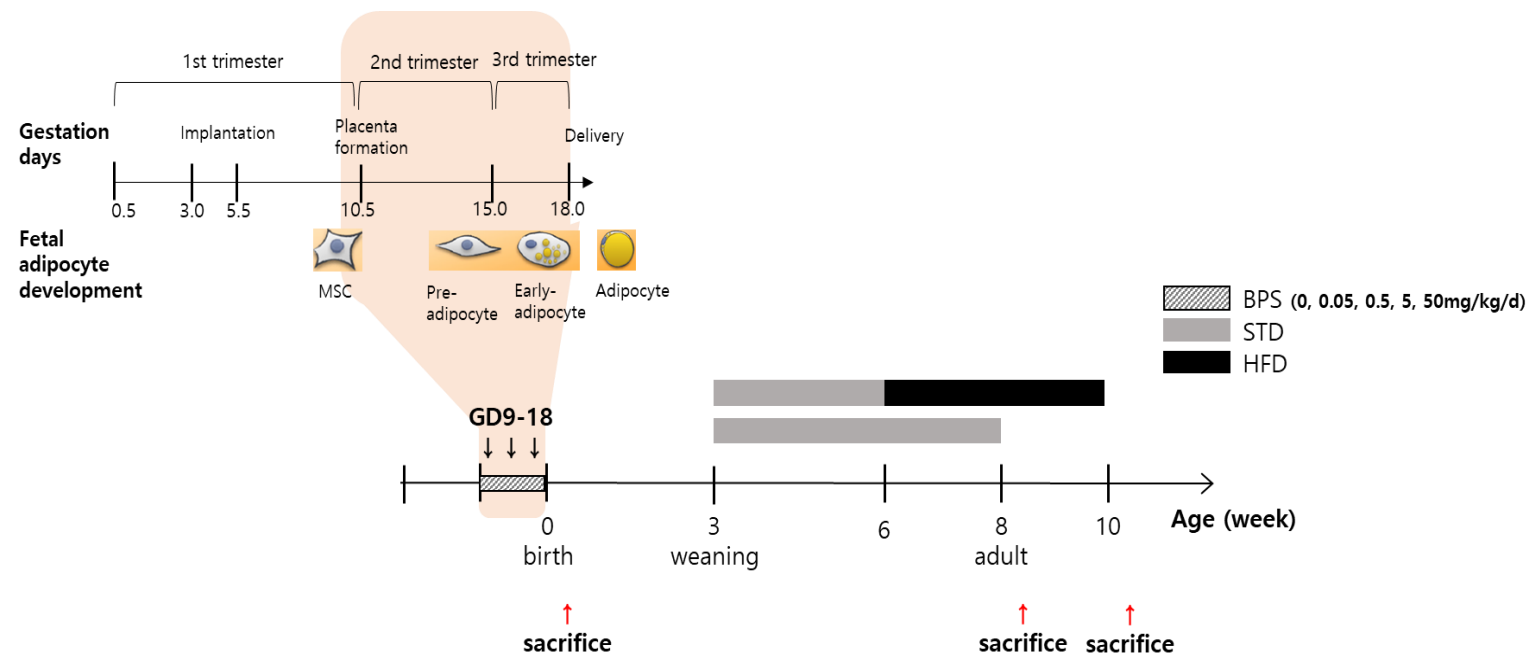


Figure 1-6. Overview of animal experiment design.

## **Chapter 2. Delivery of BPS during fetal stage F1**

### **2.1. Introduction**

As BPS is extensively used as an alternative to BPA, it has become increasingly ubiquitous in the environment (Chen et al. 2016). In food samples from the United States, BPS was detected second most frequently after BPA (21% vs. 57%) (Liao and Kannan 2013). Apart from food, BPS is also present in indoor dust as an ubiquitous contaminant (Liao et al. 2012a). Another source of exposure to BPS is thermal paper, because BPS has partially replaced BPA as a color developer (Thayer et al. 2016; Vervliet et al. 2019). In human biomonitoring data, it has been detected in over 80% of urine samples in the US (Lehmle et al. 2018) and various Asian countries (Liao et al. 2012). The detection rate of urinary BPS in adults was reported to have increased from 2000 to 2014 in the US (Ye et al. 2015). Additionally, recent studies have highlighted placental transfer of BPS. For example, BPS was detected in the urine of pregnant women in Canada (J Liu et al. 2017; Liu et al. 2018) and China (Wan et al. 2018) which implies that maternal exposure to BPS might reach fetal circulation by crossing the placenta (J Liu et al. 2017).

Exposure to BPS during fetal development can result in a range of health effects including reproductive, developmental, metabolic effects, and obesity due

to its estrogenic properties (Hill et al., 2017; Ji et al., 2013; Naderi et al., 2014; Pu et al., 2017; Qiu et al., 2016). Due to the structural similarity of BPS with BPA, *in vitro* and *in vivo* data have suggested that BPS may have endocrine disrupting effects similar to BPA (Eladak et al., 2015; Goldinger et al., 2015; Rochester and Bolden, 2015; Roelofs et al., 2015; Rosenmai et al., 2014). Evidence on the adverse effects has demonstrated that only unconjugated bisphenols (BPs) can bind to estrogen receptors (reviewed by Gramec Skledar and PeterlinMašić 2016) and hydroxylated BPS (HO-BPS) is thought to exhibit endocrine activity (Skledar et al. 2016). On the other hand, BPs-glucuronides have been found to lack estrogenic activity (Li et al. 2013; Matthewsetal.2001; Skledaretal.2016; Snyderetal.2000). Waidyanatha et al. (2018) demonstrated that the pattern of BPS metabolism was similar to BPA reported with glucuronide and sulfate as the major metabolites in both rats and mice upon the route of administration. In general, BPS is mainly metabolized in the liver into bisphenol S glucuronide (BPSG) and is eliminated in human urine (Gramec Skledar and Peterlin Mašič, 2016; Le Fol et al., 2015). BPS-sulfate (BPS-G) is also excreted in urine and feces for detoxification (Waidyanatha et al. 2018). Yet, the BPA-glucuronide (BPA-G) cannot be regarded as completely inactive, as it possibly induces adipocyte differentiation (Boucher et al. 2015). Thus, unconjugated and conjugated metabolites can be key to understand the health effects from early-life exposure to BPS.

Moreover, it is noted that fetal liver and intestine, which are too immature to

metabolize xenobiotic BPS and fetal exposure to BPS can elevate the active BPS due to de-glucuronidation. It has been known that the liver and intestine are the organs for glucuronidation of BPS by expressing metabolic enzymes such as uridine diphospho-glucuronosyltransferases (UGT) isoforms (Skledar et al. 2016). In the fetus and newborn, those enzymes may differ from the one in adults and the organs for metabolism are not fully functional. Developing organisms have an increased metabolic rate as compared to adults, which, in some cases, may result in increased toxicity. The elimination of BPS-G from the fetal compartment is difficult and leads to its back-conversion into bioactive BPS according to the ovine materno-feto-placental model (Grandin et al. 2018). Thus, remained metabolites are required to investigate in offspring maternally exposed to BPS.

This study was conducted to (1) investigate whether the offspring were exposed to BPS from maternal mice (2) identify and determine neonatal BPS metabolites remained through fetal life.

## **2.2. Materials and methods**

### **2.2.1. Chemicals and reagents**

Bisphenol S (4,4-sulfonyldiphenol, 98%) and HO-BPS were purchased from Sigma-Aldrich (St. Louis, MO, U.S.A.) and Fluorochem (Old Glossop, UK), respectively.  $^{13}\text{C}_{12}$ -labeled BPS ( $^{13}\text{C}_{12}$ -BPS), BPS-G and BPS-S (96%, Cat no. B519628, Bisphenol S Monosulfate Disodium Salt) were purchased from Toronto Research Chemicals, Inc. (Toronto, ON, Canada). Acetonitrile and methanol (HPLC grade) were obtained from Avantor (Center Velly, PA). Formic acid (98+%, pure) was obtained from Acros Organic (Geel, Belgium). Leucine enkephalin and sodium formate was purchased from Waters (Milford, USA).

### 2.2.2. Animal treatment

The animal experiments were in accordance with the guidelines of the Institutional Animal Care and Use Committee of Seoul National University (approval ID: SNU-160930-3-4). Pregnant C57BL/6N female mice at gestation day 2 (GD2) were obtained from a commercial animal breeder (Koatech, Gyeonggi-do, Korea). Polysulfone cages (GM500; Techniplast, Buggugiate, Italy) and glass water bottles (JD-C-88N; Jeung Do B&P Co. Ltd., Seoul, Korea) were used herein. BPS and absolute ethanol were purchased from Sigma-Aldrich (Saint Quentin Fallavier, France).

Fifty-seven pregnant mice aged 14–16 weeks were individually housed under standard conditions with *ad libitum* access to food and water in an environmentally controlled room and maintained on a 12:12-h light/dark cycle. From gestation day 9 (GD9), they were exposed to BPS via drinking water. The BPS doses were 0 (control), 0.2, 2.1, 21.4, and 214.3  $\mu\text{g/mL}$  (with 0.5% ethanol v/v to dissolve the crystalized BPS), which corresponded to 0 (control), 0.05, 0.5, 5, 50 mg/kg body weight/d indicates the calculated doses of BPS considering the maternal body weight). The highest BPS dose (50 mg/kg/d) was selected on the basis of no-observed-adverse-effect-levels (NOAELs) for changes in body weight ranging 40–100 mg/kg/d, which were reported on administering repeated doses of BPS to rats (ECHA 2014). The other selected doses were one-tenth those of the upper BPS dose. Since no reference dose of BPS is currently available, the lowest

dose was selected on the basis of the EPA chronic oral reference dose (RfD) for daily BPA exposure to humans (0.05 mg/kg/d) (U.S.EPA. 1988). BPS was continuously administered through drinking water until parturition (GD18).

### 2.2.3. Sample collection and preparation

Three or four dams from different cage per each exposure group are randomly selected, and their offspring are randomly extracted five per each exposure group. All samples were collected under anesthesia. For neonate's biological samples, dissected liver tissues and the rest of the body at postnatal day 1 (PND 1) were collected and immediately frozen in liquid nitrogen. All collected samples were stored in a deep freezer ( $< -70^{\circ}\text{C}$ ) until further processing.

Analysis of BPS in liver and the rest of body at PND1 was performed by following the method for global metabolome as previously described with some modifications (Want et al. 2013). Briefly, after thawing in a refrigerator ( $4-8^{\circ}\text{C}$ ), an aliquot (50~60mg) of tissues was transferred into a 2 mL polypropylene tube, homogenized using a bead-beating homogenizer, added 1 mL of pre-chilled methanol, and 20  $\mu\text{L}$  of  $^{13}\text{C}_{12}$ -BPS (2  $\mu\text{g}/\text{mL}$ ) was spiked as internal standard. The mixture was incubated in a sonication bath at  $4^{\circ}\text{C}$  for 10 min, and then centrifuged at 14,000g and  $4^{\circ}\text{C}$  for 10 min. The supernatant was transferred to a glass tube, and concentrated to near-dryness under a gentle nitrogen stream. The extract was reconstituted with 50  $\mu\text{L}$  of mobile phase, vortex mixed, and transferred into an auto-sampler vial for injection to UPLC-qTOF/MS.

The details of the method for tissue homogenization is as follows: To minimize potential changes in sample composition before solvent extraction, tissue



was thawed on ice before sample preparation. Further, a weighed amount of the tissue (50~60mg) is homogenized in order to enable good access of the extracting solvent to the tissue. Weighted tissues were transferred to a 2mL-Eppendorf tube containing a stainless steel bead (5-mm I.D). For liver tissue, mechanical disruption using a bead-beating homogenizer was used. For whole body tissue, manual disaggregation of cold tissue (0-4°C) with scissors was performed before mechanical disruption since body skin was difficult to homogenize. The bead-beating homogenizer was operated twice at 25Hz for 2.5 minutes.

#### 2.2.4. Instrument analysis

UPLC-ESI-QTOF/MS analysis was performed on an ACQUITY™ UPLC system (Waters Corp., Milford, MA, USA) interfaced with a Waters Synapt G2-Si QTOF MS with electrospray ionization (ESI) operated in the negative ion mode. The capillary voltage was 2.5 kV, and the cone voltage was 30V. The source temperature was set at 100°C with a cone gas flow rate of 50 L/h, a desolvation gas temperature of 250°C, and a nebulization gas flow of 600 L/h. Both the cone gas and the nebulization gas were nitrogen. The instrument was operated in resolution mode and was set to acquire data over the  $m/z$  range of 50–1200 with a scan time of one second. All mass spectral data were collected in profile mode using the MSE data acquisition function to simultaneously obtain fragmentation data. In function one, a low collision energy (6 eV) was used, and in the second function, a high collision energy (ramp 10–40 eV) was used for fragmentation.

Leucine-enkephalin ( $m/z$  554.2615 for the negative ion mode) was used as a reference mass at a concentration of 1 ng/mL in 50% acetonitrile containing 0.1% formic acid infused at a flow rate of 10  $\mu$ L/min via a lock spray interface. Reference mass scans were collected every 10 seconds and required over 3 scans on average to perform mass correction. Sodium formate was used to set up mass spectrometer calibration in negative ion mode before sample analyses.

The method of UPLC separation was adopted and modified from the protocols for global metabolomics by Saigusa et al. (2016). UPLC separation was

achieved on a Waters ACQUITY™ UPLC BEH C18 column (100 × 2.1 mm, 1.7 μm) with the column temperature set at 40 °C. The mobile phase consisted of (A) water containing 0.1% formic acid and (B) acetonitrile containing 0.1% formic acid. The following solvent gradient was applied: The initial condition was set at 1.0% B. The following solvent gradient was applied: 1.0% B for 1 min followed by a linear gradient to 99% B from 1 to 8 min, and then 85% B for 5 min. Subsequently, the mobile phase was immediately returned to the initial conditions and maintained for 2 min until the end of the run. The flow rate was 0.4 mL/min, injection volume was 5 μL.

The analysis data were collected using MassLynx v4.1 software with MS<sup>E</sup> program (Waters Corp., Manchester, UK).

Table 2-1. Instrument condition

<b>UPLC</b>	<b>Instrument</b>	Waters Synapt G2-Si QTOF MS
	<b>Inject volume</b>	5 µl
	<b>Flow rate</b>	0.4ml/min
	<b>Oven temp</b>	40°C
	<b>Column</b>	ACQUITY UPLC BEH (C18, 1.7 µm , 2.1x100mm)
	<b>Mobile phase (A)</b>	0.1% formic acid in water
	<b>Mobile phase (B)</b>	0.1% formic acid in acetonitrile
<b>QTOF/MS</b>	<b>ESI</b>	Negative ion mode
	<b>Analyzer mode</b>	Resolution
	<b>TOF-MS</b>	MS <sup>E</sup>
	<b>Scanning condition</b>	Continuum
	<b>Collision Energy</b>	Low energy: 6V
		High energy: Ramping from 10 to 40V
	<b>Cone Voltage</b>	40V
	<b>Total run time</b>	20 minutes

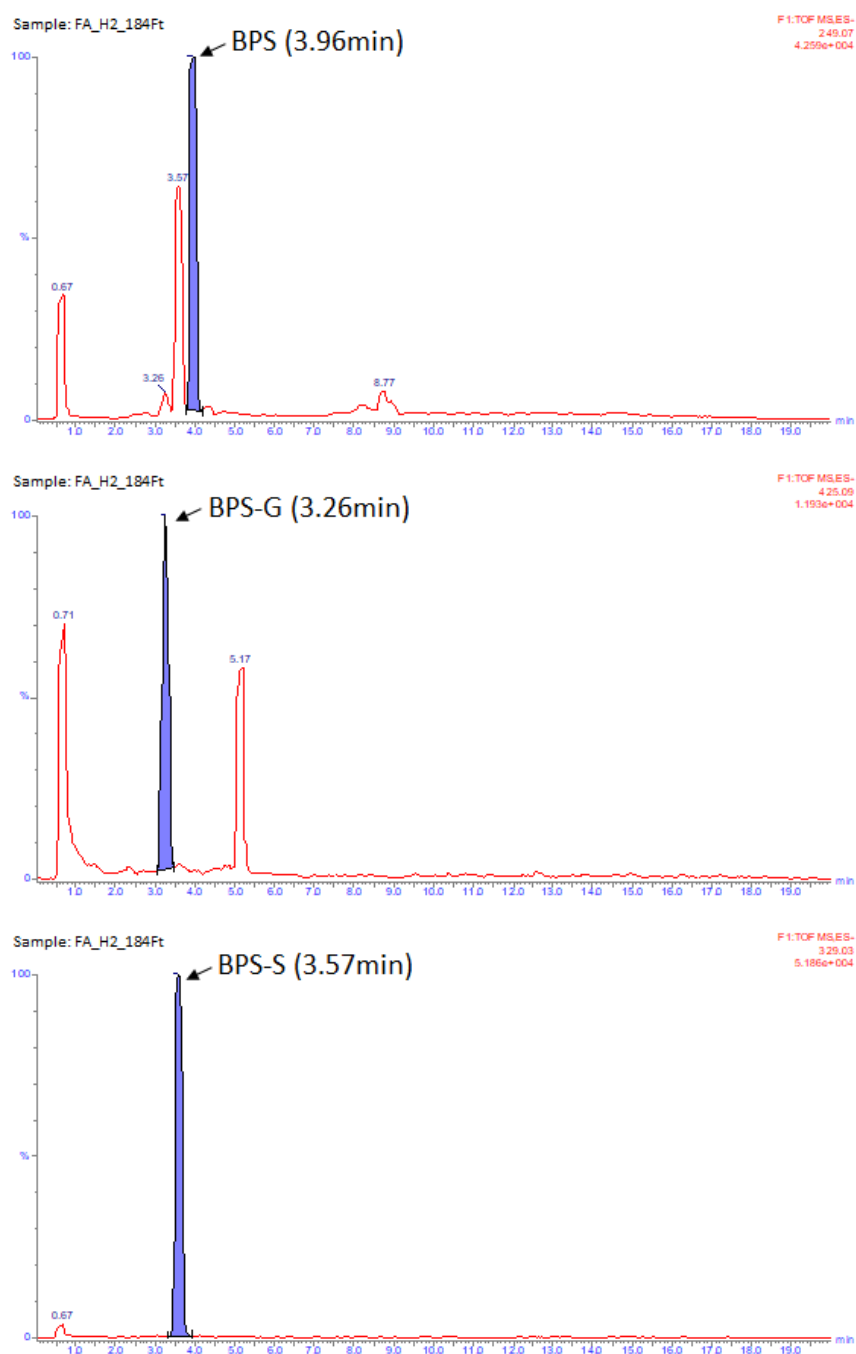


Figure 2-1. Chromatogram of BPS metabolites in the rest of body of PND1.

Table 2-2 Accurate m/z ratio of the [M-H]<sup>-</sup> precursor ions, total fragment ions found by MS/MS

<b>BPS metabolites</b>	<b>RT(min)</b>	<b>[M-H]<sup>-</sup></b>		<b>Total fragment ions</b>	
		<b>Precursor</b>	<b>Target ion</b>	<b>Confirmation ion</b>	
<b>free-BPS</b>	3.96	249.017	108.017	155.983	92.023
<b>HO-BPS</b>	3.65	265.011	124.010	156.989	108.017
<b>BPS-G</b>	3.26	425.043	249.017	113.018	175.016
<b>BPS-S</b>	3.57	329.880	248.962	107.990	155.946

#### 2.2.5. Quality assurance (QA) and quality control (QC)

For each batch of 20 samples, a method blank, and a pair of matrix-spiked (QC check) samples were analyzed. To prevent possible contamination, we washed all glassware materials used for pretreatment with detergent and rinsed with Milli-Q water, methanol and acetone.

QC samples and calibration curves for measurement of BPS in biological media were constructed with method blanks – pooled extra liver and the rest of body from offspring at PND 1 in the non-exposure group. A 50mg of pooled extra tissues was homogenized with 1 mL of pre-chilled methanol. Analytical standard solutions (50  $\mu$ L) was spiked in the method blank, yielding final calibration concentrations of 0.1, 0.25, 0.5, 1.0 and 2.5 ng/mg wet weight of tissue. Internal standard (20  $\mu$ L) containing the  $^{13}\text{C}_{12}$ -BPS in methanol at a concentration of 2  $\mu$ g/mL was added to all samples. Calibration curve was plotted based on a ratio of the peak area of analytical standard to internal standard, whose regression coefficient ( $R^2$ ) was represented in Table 2-3. The limit of detection (LOD) was calculated as  $3s_a/b$ , where  $s_a$  is the standard deviation of the response and  $b$  is the slope of the calibration curve, the lower limit of quantitation (LLOQ) was calculated as  $5s_a/b$ , and the limit of quantitation (LOQ) was calculated as  $10s_a/b$ . The LOD, LLOQ and LOQ were represented in Table 2-4 and Table 2-5. BPS was not detected or ignorable (less than LODs) in the methods blanks.

Table 2-3. Calibration curve and the regression coefficient ( $R^2$ )

<b>BPS metabolites</b>	<b>Liver</b>		<b>The rest of body</b>	
<b>free-BPS</b>	$y = 0.5002x + 0.0144$	$R^2 = 0.9991$	$y = 0.2472x - 0.0096$	$R^2 = 0.99$
<b>HO-BPS</b>	$y = 0.2595x - 0.0201$	$R^2 = 0.9953$	$y = 0.0825x - 0.004$	$R^2 = 0.9958$
<b>BPS-G</b>	$y = 0.1042x - 0.0107$	$R^2 = 0.9942$	$y = 0.0198x - 0.0009$	$R^2 = 0.9929$
<b>BPS-S</b>	$y = 0.3979x - 0.022$	$R^2 = 0.9991$	$y = 0.4434x - 0.038$	$R^2 = 0.9874$

Table 2-4. LOD, LLOQ and ULOQ in liver at PND1

<b>BPS metabolites</b>	ng/g, wet wt.		
	<b>LOD</b>	<b>LLOQ</b>	<b>ULOQ</b>
<b>free-BPS</b>	47.7	79.5	159.0
<b>HO-BPS</b>	110.8	184.7	369.4
<b>BPS-G</b>	123.9	206.5	412.9
<b>BPS-S</b>	45.8	76.3	152.5

Table 2-5. LOD, LLOQ and ULOQ in the rest of body at PND1

<b>BPS metabolites</b>	ng/g, wet wt.		
	<b>LOD</b>	<b>LLOQ</b>	<b>ULOQ</b>
<b>free-BPS</b>	99.8	151.2	302.4
<b>HO-BPS</b>	60.4	91.5	183.0
<b>BPS-G</b>	84.0	127.3	254.6
<b>BPS-S</b>	112.0	169.7	339.4



#### 2.2.6. Calculation of $\Sigma$ BPS metabolites

Using the molecular weight of each metabolite,  $\Sigma$  BPS metabolites were calculated by summing up the amounts.

$$\Sigma \text{ BPS metabolites} = \text{free BPS} + \text{HO-BPS} + \text{BPS-G} + \text{BPS-S}$$

## **2.3. Results**

### **2.3.1. Determination of BPS metabolites at PND 1**

The concentration and detection rate of four BPS metabolites at PND 1 are represented in Table 2-6.

#### **(1) BPS metabolites in liver tissues at PND 1**

Free-BPS and BPS-S were detected in all liver tissue samples. A peak of HO-BPS was traced in chromatography, but the level was less than LOD. BPS-G were not detected in all liver tissues tested. Two BPS metabolites were quantified only in BPS 50 mg/kg/d. The peaks of free-BPS were traced in BPS 5 mg/kg/d, but it was less than LOD. The concentration of free-BPS in 50 mg/kg/d groups was ranged from <LOD to 132.6 ng/g tissue. The peaks of BPS-S were traced in BPS 0.5 and 5 mg/kg/d, but the concentration was less than LOD. The concentration of BPS-S in 50 mg/kg/d groups was ranged from 90.1 to 150.8 ng/g tissue. BPS-S was predominant, followed by free BPS. (BPS-S > free-BPS)

#### **(2) BPS metabolites in liver tissues at PND 1**

The concentration of BPS metabolites was determined only in BPS 50 mg/kg/d. The detection rate of free-BPS, BPS-G and BPS-S were 40%, 100% and 60%, respectively. OH-BPS was less than LOD in all samples. Of four metabolites, only BPS-S was traced in the group of BPS 0.5 and 5 mg/kg/d, but less than LOD. In BPS 50 mg/kg/d, the levels of free BPS were ranging from <LOD to 365.0 ng/g tissue, BPS-G was from 108.8 to 438.9 ng/g tissue, and BPS-S ranged from <LOD to 203.9 ng/g tissue. BPS-G was the most abundant, followed by free-BPS and BPS-S. (BPS-G > free-BPS > BPS-S)

#### **2.3.2. Sum of BPS metabolites remained at PND 1**

The sum of amount of BPS metabolites except BPS-G was 32.7 nmol in liver samples. The sum of amount of BPS metabolites was 73.8 nmol in the rest of body. (see Table 2-7).

Table 2-6. Concentration and detection rates of BPS metabolites at PND1 (n=5)

<b>BPS metabolites (ng/g, wet weight)</b>	<b>Liver</b>				<b>The rest of body</b>			
	<b>Mean</b>	<b>SD</b>	<b>Range</b>	<b>Detection rate (%)</b>	<b>Mean</b>	<b>SD</b>	<b>Range</b>	<b>Detection rate (%)</b>
<b>free-BPS</b>	69.8	40.6	<47.7 - 132.6	60	156.5	139.9	<99.8 - 365.0	40
<b>HO-BPS</b>	<110.8	-	-	-	<60.4	-	-	-
<b>BPS-G</b>	N.D.	-	-	-	193.3	139.7	108.8 - 438.9	100
<b>BPS-S</b>	123.6	25.4	90.1 - 150.8	100	130.6	59.6	<112.0 - 203.9	60
<b>Σ BPS metabolites</b>	193.4				480.4			

Note. Maternal applied dose of BPS, 50mg/kg/day. N.D. not detected

Table 2-7. The sum of amount of BPS metabolites at PND 1 (n=5)

<b>BPS metabolites (nmol)</b>	<b>Liver</b>		<b>The rest of body</b>	
	<b>Mean</b>	<b>SD</b>	<b>Mean</b>	<b>SD</b>
<b>free-BPS</b>	14.0	8.1	31.3	28.0
<b>HO-BPS</b>	<14.8	-	<11.4	-
<b>BPS-G</b>	N.D	-	22.7	16.4
<b>BPS-S</b>	18.7	3.8	19.8	9.0
<b>Σ BPS metabolites</b>	32.7		73.8	

## **2.4. Discussion**

By detecting BPS raw materials and metabolites in the PND1 biological sample, it can be confirmed that BPS was transmitted from the mother. Summarizing the early exposure characteristics, free BPS and BPS conjugates were detected in non-liver samples. I would like to consider the results of this study by comparing metabolism characteristics (including differences in metabolic function maturity-age differences, species differences) and BPA metabolic characteristics.

Furthermore, through in vitro studies that reveal BPA-G is no longer considered inactive, and affects adipogenesis, the effect of BPS exposure on adiposity at the time of fat differentiation can be seen as an explainable link in addition to epigenetic programming. The fact that BPSG was not detected at low concentrations of exposure can also be explained as a technical issue of the detection limit, but adiposity effects at low concentration can be explained by epigenetic change, and adiposity effects at high concentration can be explained by BPSG generation and adipogenesis.

The BPS metabolite detection rate was high even after 1 day of exposure. It clearly shows the delivery of BPS from the mother, and, given that the half-life of BPS is less than 10 hours, excessive accumulation can be expected. In addition, pregnant mice may show rapid discharge when exposure is stopped, but in the case of a fetus, exposure of pregnant mothers may be associated with vulnerability for

exposure of the fetus because it may be difficult to expect rapid discharge due to underdeveloped metabolic functions and immature metabolism.

The sum of BPS metabolites accounted for 14.6 % of the mother's exposure after 1 day of discontinuation. Although the total BPS was not measured, it can be seen that the body burden of PND1 is greater than that of the mother. Even if exposed to BPS, which is known to have a relatively short half-life, at least 32.7 nmol to 73.8 nmol of BPS per gram remain. It can be seen that when the pregnant mouse is continuously exposed to 50 mg/kg/d during pregnancy, F1 is born with a body burden of 500 ppb or more. Repeated exposure to the BPA repeated exposure of pregnant mice showed that the pattern of BPA concentration in the mother's blood and liver decreased after a certain period of time after 10 mg/kg administration, while the fetus repeated BPA whenever the administration was repeated (Kawamoto et al. 2005). It can be seen that it tends to accumulate. Also, a study of BPS in pregnant sheep model has been reported that proportion of BPS-G in fetus crossing placenta was small but excretion rate was low (Grandin et al. 2018). Therefore, it can be guessed that excessive accumulation of BPS in the midst of the present study is also seen as a result of detection even after 1 day of stopping the exposure.

In the highest exposure group (BPS 50 mg/kg/d), free-BPS, BPS-G, and BPS-S were still detectable one day after birth. Interestingly, BPS-G was not detected in liver tissue. The results show that the liver as a main organ of metabolism was likely immature and metabolic enzymes differ from adults, and

that they may still be trapped because they do not cross the placenta barrier.

Early-life exposure to BPA through the mother has been demonstrated by the detection of BPA raw materials and BPA-G in neonatal biological samples or cord blood (Lee et al. 2018). However, the mainstream theory is that the metabolite BPA-G produced by the mother is a substance with a large molecular weight that is difficult to pass through the placenta. This makes it unlikely to be transmitted to the fetus as it is. On the other hand, some studies have looked at aspects of early exposure and metabolic characteristics. When the mother is exposed to BPA, it can be seen that BPA and its metabolites are detected in the child's biological sample. One is that only the BPA raw material is delivered from the mother and immature but produces BPA-G because it undergoes phase II metabolism in sheep (Gauderat et al. 2016). In another opinion, the form that the pregnant sheep is exposed to BPA, metabolizes rapidly, and can be transmitted to the placenta is BPA-G. It has been reported that when BPA-G is transmitted through the placenta in a sheep model, free-BPA forms can also be detected through de-conjugation (Corbel et al. 2015).



## **Chapter 3. Adipogenic effects of prenatal exposure to BPS in adult F1 male mice**

### **3.1. Introduction**

The use of “BPA-free” products including polycarbonate bottles, canned food linings, and thermal paper has increased, since numerous studies have reported the deleterious effects of bisphenol A (BPA). Although BPA is still used in industries, numerous bisphenol analogs are commercially available worldwide, among which, BPS has been increasingly used; however, no evidence is available to show that BPS is less toxic than BPA (Chen et al. 2016; Lee et al. 2017; Oh et al. 2018; Silva et al. 2019).

BPS has been detected in both environmental and biological samples. Furthermore, BPS is reportedly consumed through the diet worldwide and is present in various environmental matrices (Eckardt and Simat 2017; Liao and Kannan 2013, 2014; Liu et al. 2018; Yan et al. 2017). The widespread adoption of BPS has been further confirmed through its detection in >80% of human urine samples in the US (Lehmle et al. 2018) and Saudi Arabia (Asimakopoulos et al. 2016). Moreover, urinary BPS has been detected in pregnant women in Canada (J Liu et al. 2017; Liu

et al. 2018) and China (Wan et al. 2018), raising the concern that maternal exposure to BPS can lead to fetal exposure if BPS crosses the placenta and enters fetal circulation (J Liu et al. 2017). Furthermore, in cross-sectional studies, BPS levels were higher among obese rather than in non-obese adults in the US (B Liu et al. 2017; Liu et al. 2019).

Increasing concerns have emerged regarding the association between the exposure to endocrine disrupting chemicals (EDCs) including bisphenol analogs and various pathologies including obesity and metabolic disorders, developmental and reproductive abnormalities, thyroid-related disorders, and cancers (WHO 2018; WHO/UNEP 2013). Recent literature reviews have reported that certain obesogenic EDCs may regulate and promote lipid accumulation and adipogenesis (Darbre 2017; Grun and Blumberg 2009; Heindel et al. 2015; Sidhu et al. 2000; Veiga-Lopez et al. 2018). Several studies on the obesogenic properties of BPA analogs have focused on the nuclear receptor (NR)-related mechanism of adipose tissue function (Ahmed and Atlas 2016; Ariemma et al. 2016; Boucher et al. 2016b; Vom Saal et al. 2012).

Owing to the structural similarity of BPS and BPA, numerous health scientists have investigated whether BPS causes any deleterious effects comparable to those of BPA. A recent study reported that BPS induced adipogenesis *in vitro* by targeting peroxisome proliferator-activated receptor gamma (*Pparg*), a key regulator of adipogenesis, and its downstream target genes in primary human preadipocytes, murine 3T3-L1 preadipocytes, and swine adipose stromal cells

(Berni et al. 2019; Boucher et al. 2016a; Helies-Toussaint et al. 2014) similar to BPA (Ahmed and Atlas 2016). Another study reported that BPS interacts with estrogen receptor alpha (ER $\alpha$ ) in human cell lines MCF-7 and HepG2 (Li et al. 2018) and induced estrogenic activity (Ng et al. 2015) comparable to that of BPA. BPS reportedly causes adipocyte-specific transcriptional changes earlier than BPA and alters the expression of genes specifically associated with adipogenesis and lipid metabolism in human primary preadipocytes (Boucher et al. 2016b). Numerous studies have reported the short-term effects of BPS exposure on adult murine/human preadipocytes.

Based on the developmental origins of health and disease (DOHaD) concept (Barrett 2017; Breton et al. 2017; Yamada and Chong 2017), early-life environmental exposure, especially *in utero*, potentially contributes to metabolic and cardiovascular diseases in later life (Armitage et al. 2008). Although existing human data on BPA and metabolic diseases are limited, prenatal exposure to BPA is reportedly associated with the pathogenesis of metabolic diseases including obesity and diabetes in adult offspring (Alonso-Magdalena et al. 2010; Vom Saal et al. 2012; Wassenaar et al. 2017).

In addition to the recently reported effects of early-life BPS exposure, additional information is required regarding the role and temporal effects of BPS either as an obesogen *per se* or stimulator prone to obesity. A few *in vivo* studies reported the adiposity-related effects of BPS exposure during development (da

Silva et al. 2019; Ivry Del Moral et al. 2016; Pu et al. 2017). In terms of the susceptible period of exposure, however, it is unclear whether adiposity in later life is affected by prenatal or perinatal BPS exposure. For instance, a perinatal exposure study using a sheep model investigated the adipogenic effects of BPS exposure during fetal development; however, they did not observe phenotypic changes in later life (Pu et al. 2017).

To elucidate the inclusive findings of these previous studies and to address the knowledge gap on the susceptibility window for BPS exposure, this study investigated the effects of prenatal BPS exposure on adiposity in adult mice.

## 3.2. Materials and methods

### 3.2.1. Animal treatment

The animal experiments were in accordance with the guidelines of the Institutional Animal Care and Use Committee of Seoul National University (approval ID: SNU-160930-3-4). Pregnant C57BL/6N female mice at gestation day 2 (GD2) were obtained from a commercial animal breeder (Koatech, Gyeonggi-do, Korea). Polysulfone cages (GM500; Techniplast, Buggugiate, Italy) and glass water bottles (JD-C-88N; Jeung Do B&P Co. Ltd., Seoul, Korea) were used herein. BPS and absolute ethanol were purchased from Sigma-Aldrich (Saint Quentin Fallavier, France). The pregnant mice and a group of F1 offspring were administered standard diets (STD; NIH41; Zeigler Bros. Inc., Gardners, PA, USA) until euthanasia, and the other F1 offspring were administered standard diets, followed by high-fat diets (HFD; 60% kcal fat; D12492, Research Diet Inc., New Brunswick, NJ, USA) for 4-week high-fat challenge 6 weeks postpartum until euthanasia.

Fifty-seven pregnant mice aged 14–16 weeks were individually housed under standard conditions with *ad libitum* access to food and water in an environmentally controlled room and maintained on a 12:12-h light/dark cycle. From gestation day 9 (GD9), they were exposed to BPS via drinking water. The BPS doses were 0 (control), 0.2, 2.1, 21.4, and 214.3 µg/mL (with 0.5% ethanol v/v to dissolve the crystalized BPS), which corresponded to 0 (control), 0.05, 0.5, 5, 50

mg/kg body weight/d (Table 3-1 indicates the calculated doses of BPS considering the maternal body weight). The highest BPS dose (50 mg/kg/d) was selected on the basis of no-observed-adverse-effect-levels (NOAELs) for changes in body weight ranging 40–100 mg/kg/d, which were reported on administering repeated doses of BPS to rats (ECHA 2014). The other selected doses were one-tenth those of the upper BPS dose. Since no reference dose of BPS is currently available, the lowest dose was selected on the basis of the EPA chronic oral reference dose (RfD) for daily BPA exposure to humans (0.05 mg/kg/d) (U.S.EPA. 1988). BPS was continuously administered through drinking water until parturition (GD18). Furthermore, we also ensured the absence of BPS contamination in drinking water and cages by weekly monitoring drinking water and cage swabs. BPS was quantified using the method of Oh et al. (2018)) with minor modification, using the API 4000 electrospray triple quadrupole mass spectrometer (ESI-MS/MS; AB SCIEX, Framingham, MA, USA), coupled with a Nexera HPLC system (Shimadzu, Kyoto, Japan). Experimentally calculated concentration of BPS in drinking water was  $0.00 \pm 0.02 \mu\text{g/mL}$  (n=6). BPS from cage swabs was not detected. Water and food consumption were recorded on a weekly basis. No significant difference in water intake was observed in BPS-treated mice (of all doses) and vehicle control mice (data not shown).

A representation of the experimental design and number of study animals are provided in Figure 3-1 and Table 3-2, respectively. The birth weights of the

offspring were measured daily. The offspring were housed with their mothers until weaning (postnatal day 21). Thereafter, the offspring were first segregated by sex, and then further divided into groups for each diet (STD and HFD) at a sexually mature age (6 weeks of age). An HFD was administered (Podrini et al. 2013) for 4 weeks as a high-fat challenge to stimulate adipogenesis, while STD-fed mice were euthanized at approximately 8 weeks of age. Maximum four mice were housed in a cage. To minimize potential sibling effects, the litters were randomly mixed after weaning. To harvest tissue specimens, the mice were anesthetized through 0.5–2% isoflurane (Forane Sol®, Choongwae Pharm Co., Seoul, Korea) inhalation after 6 h of fasting.

Table 3-1. Applied doses of bisphenol S adjusted to the maternal body weight

Exposure group	Expected dose of BPS	BPS in water <sup>a</sup>	Dams at GD16		Calculated dose of BPS <sup>c</sup>
	(mg/kg/d)	(µg/mL)	N	Body weight (g) <sup>b</sup>	(mg/kg/d)
<b>Vehicle control</b>	<b>0</b>	0	16	28.86 ± 4.41	0.00
<b>BPS</b>	<b>0.05</b>	0.214	8	26.17 ± 1.10	0.05 ± 0.00
	<b>0.5</b>	2.143	4	26.01 ± 3.31	0.50 ± 0.06
	<b>5</b>	21.43	12	26.40 ± 2.72	4.92 ± 0.47
	<b>50</b>	214.3	17	29.28 ± 5.17	44.98 ± 6.28

<sup>a</sup> It represented theoretically calculated concentration of BPS in drinking water.

<sup>b</sup> Maternal body weights were recorded at gestational day 16.

<sup>c</sup> The calculations assumed that 6 mL/day of water would be consumed.  
BPS, bisphenol S.

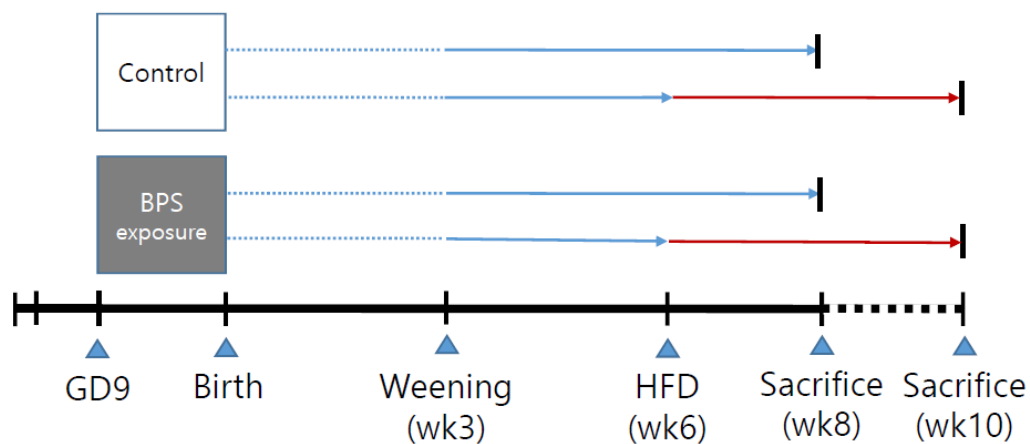


Figure 3-1. Schematic representation of the experimental protocol. BPS, bisphenol S; STD, standard diet; HFD, high-fat diet; GD, gestational day.

Table 3-2. The number of dams and male offspring in the bisphenol S exposure group

Exposure (mg/kg/d)	Dams	Male offspring at sacrifice		
	N	N <sub>STD</sub>	N <sub>HFD</sub>	N <sub>Total</sub>
<b>Control</b>	16	13	16	29
<b>BPS 0.05</b>	8	6	6	12
<b>BPS 0.5</b>	4	3	4	7
<b>BPS 5</b>	12	13	8	21
<b>BPS 50</b>	17	19	10	29
<b>Total</b>	57	54	44	98

[Notes] STD – Standard diet; HFD – High-fat diet; Control – Vehicle control



### **3.2.2. Measurement of the body weight and fat pad mass of the offspring**

To assess adiposity phenotypes in the offspring, body weight and dissected fat pad masses, including gonadal white adipose tissue (gWAT), were measured at euthanasia. Thereafter, the excised gWAT was frozen in liquid nitrogen and stored at -70 °C for further analysis (Chusyd et al. 2016). Based on previous studies on early-life BPS exposure in male mice (Ivry Del Moral et al. 2016; Meng et al. 2019; Pu et al. 2017), we decided to focus on male measures for further analysis.

### 3.2.3. Measurement of food intake and energy expenditure

To better understand the effect origins of prenatal exposure to BPS under high-fat challenge, food intake and energy expenditure were measured. Indirect calorimetry (TSE Phenomaster, Bad Homburg, Germany) was performed for randomly selected mice in each group including a vehicle control after administering an HFD ( $n = 15$ ). Approximately 10-week-old mice were individually assessed in a metabolic chamber for 48 h after acclimation over 3 d, with ad libitum access to food and water throughout the testing duration. Food intake was determined using high-precision weighing sensor-associated feeding stations. Data on oxygen consumption (ml/h per kg;  $\text{VO}_2$ ) and carbon dioxide production (ml/h per kg;  $\text{VCO}_2$ ) were curated through the oxygen ( $\text{O}_2$ ) and dioxide ( $\text{CO}_2$ ) sensors in the chamber. Energy expenditure was recorded as heat production based on the respiratory exchange rate ( $\text{RER} = \text{VCO}_2/\text{VO}_2$ ). Thereafter, we adjusted the energy expenditure to the metabolic body size (total lean mass + 0.2 total fat mass) (Even and Nadkarni 2012). Total fat and lean mass were determined in live mice on an HFD through nuclear magnetic resonance (NMR) (Minispec LF50/mq 7.5 NMR analyzer; Bruker Optics, The Woodlands, TX, USA).

#### 3.2.4. **Histological analysis of the gWAT**

To obtain phenotypic evidence regarding the effect of BPS on adipocyte hypertrophy, histological analysis was performed for the gWAT in the HFD-fed F1 male mice selected for the aforementioned energy expenditure assay. The gWAT sections were dissected out and embedded in paraffin and then stained with hematoxylin-eosin (H&E) with standard procedures. Stained slides were scanned digitally using Pannoramic Scan (3D HISTECH, Budapest, Hungary). Photographs were obtained from scanned slides at  $\times 100$  magnification and analyzed using Image Pro software (Media Cybernetics, Rockville, MD, USA) to determine the adipocyte size ( $n = 45$  images: three mice per exposure group, three sections per mouse, three fields per section). Only the interior regions of the adipocytes were selected by applying the “smart” option in the software. Adipocyte area and diameter were determined using the “count” function.

### 3.2.5. Reverse- transcription quantitative PCR analysis

To determine whether adipogenesis markers were expressed in the gWAT in all exposure and control groups of the F1 male progeny, except for those selected for histological analysis, gonadal fat pad tissues were washed in physiological saline buffer and immediately frozen in liquid nitrogen and then homogenized using a bead-beater (MN200; Retsch, Haan, Germany). Total RNA was isolated using the RNeasy Lipid Tissue Mini Kit (QIAGEN, Hilden, Germany) in accordance with the manufacturer's protocol. Total RNA purity was determined on the basis of the  $A_{260}/A_{280}$  ratio, using a Biotek Epoch Gen5 Take3 Module (Biotek, Winooski, VT, USA). cDNA as synthesized from 1  $\mu$ g of total RNA using the High-Capacity cDNA Reverse Transcription Kit (Applied Biosystems, Foster City, CA, USA), and then 1  $\mu$ L of diluted cDNA was amplified using the Power SYBR Green PCR Master Mix (Applied Biosystems). Primer sequences for the five selected genes (*Pparg*, *Cebpa*, *Fabp4*, *Lpl* and *Adipoq*) and the two housekeeping genes (*Actb* and *Eef2*) are listed in Table 3-3. cDNA amplification and quantification were performed using the QuantStudio™ 6 Flex Real-Time PCR system (Applied Biosystems). Thermal cycling was conducted using the default conditions of the QuantStudio™ Real-Time PCR Software v1.3 (Applied Biosystems) as follows: 95 °C for 10 min, followed by 40 cycles at 95 °C for 15 s and 60 °C for 1 min. All experiments were performed at least thrice, in duplicate. A threshold cycle (*Ct* value) was obtained for each amplification curve and the  $\Delta C_t$  value was first determined

by subtracting the *Ct* value for *Actb* (internal control) from the *Ct* value for each sample. Fold changes compared with the vehicle control were then determined using the  $2^{-\Delta\Delta C_t}$  method.

Table 3-3. Primers for quantitative reverse-transcription PCR analysis

Classification	Genes	Primers	Sequences
Target genes	<i>Pparg</i>	Forward	ATGACCAGGGAGTTCCTCAAAAG
		Reverse	TGCAGCAGGTTGTCTTGGATG
	<i>Cebpa</i>	Forward	AAGAGCCGAGATAAAGCCAAAC
		Reverse	AATCTCCTAGTCCTGGCTTGC
	<i>Fabp4</i>	Forward	CCGAGATTTCTTCAAACCTGGG
		Reverse	GGAAGTCACGCCTTTCATAACAC
	<i>Lpl</i>	Forward	AGAACATTCCCTTCACCCTGC
		Reverse	GCACAGAAGATGACCTTTTCTGAG
	<i>Adipoq</i>	Forward	CAAAAGGGCTCAGGATGCTACTG
		Reverse	AGAAGACCTGCATCTCCTTTCTCTC
Housekeeping genes	<i>Actb</i>	Forward	ATGAAGTGTGACGTTGACATCCG
		Reverse	TGGACAGTGAGGCCAGGATG
	<i>Eef2</i>	Forward	ATCCAGTGTCTGAGCAAGTG
		Reverse	TCAAAAGGATCCCCAGGCAG

<sup>a</sup> reverse-transcription quantitative polymerase chain reaction.

### 3.2.6. Statistical analysis

All data are expressed as mean  $\pm$  standard deviation (SD) values. Differences in the sample group means were analyzed using the *t*-test or one-way Analysis of Variance (ANOVA) with Tukey's adjustment. In the preliminary analysis, the contribution of the dam's body weight to the ones of the corresponding offspring was evaluated; however, since no such significant effect was observed, it was not considered for further analysis. Generalized linear models were constructed to evaluate the effects of BPS exposure and diet on health outcomes and for multiple comparisons among the least-square (LS) means. Multiple group comparisons were performed with *a priori* contrast tests, which was also used to test linearity with Proc GLM of SAS 9.3 (SAS Institute Inc, Cary, NC, USA). Graphical analyses were performed using R (version 3.5.1) and RStudio (version 1.1.463) with the "tidyverse" package.

### **3.3. Results**

#### **3.3.1. Body weight and fat mass**

According to an *a priori* contrast test, increases in body weight (BW) and gWAT relative to BW (gWAT/BW) followed linear trends with dosage under the high-fat challenge (Figure 3-2;  $p = 0.014$  for BW,  $p = 0.0036$  for gWAT/BW); however, these patterns were not reproduced in STD-fed mice. The LS-means of the phenotypes significantly increased from 5 mg/kg/d ( $p = 0.0036$  for BW,  $p = 0.0018$  for gWAT/BW) although no significant change in the ratio of fat mass to body weight (%) was observed upon BPS exposure (Figure 3-3).

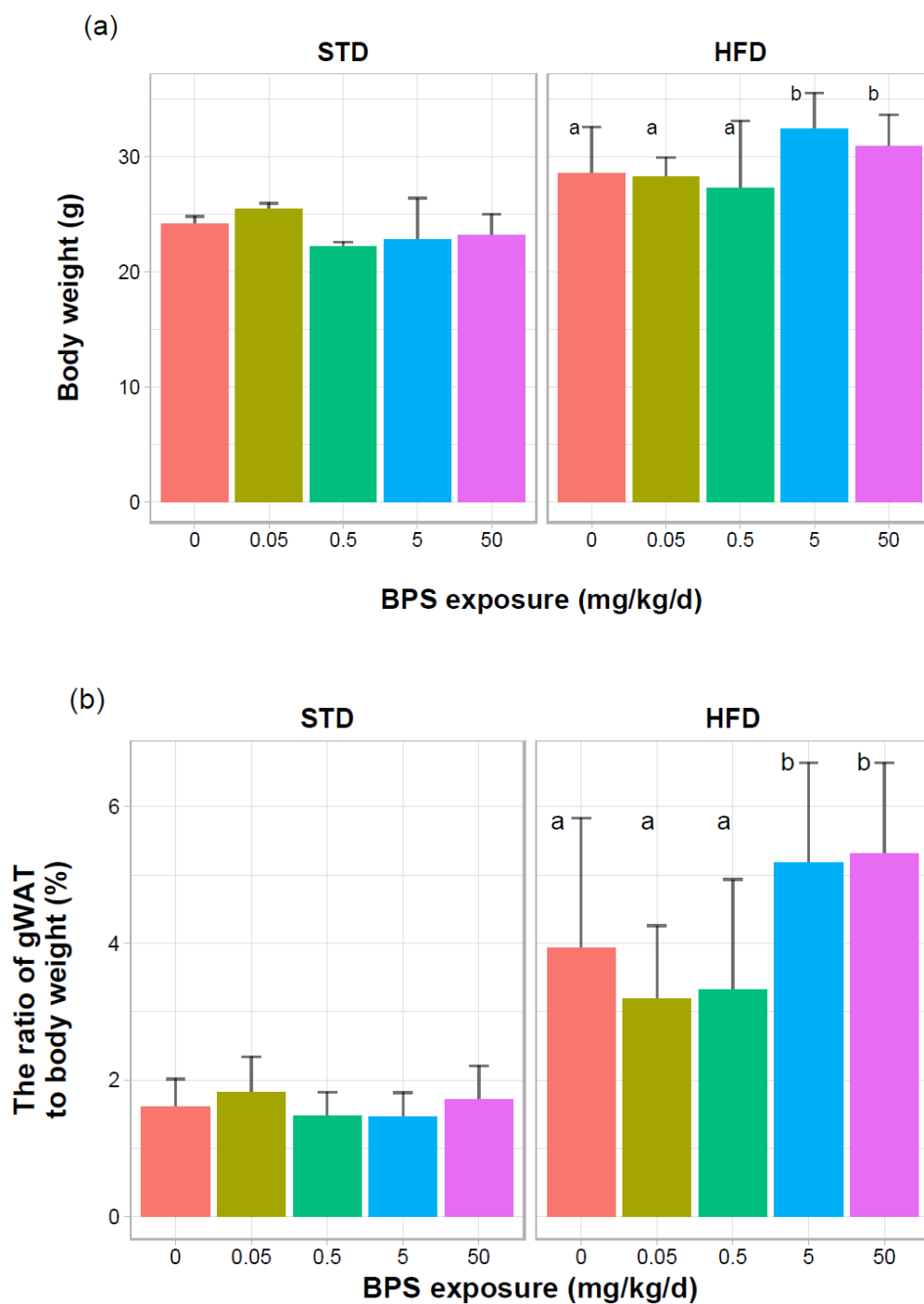


Figure 3-2. Effects of prenatal exposure to bisphenol S on body weight and the ratio



of gonadal white adipose tissue (gWAT) to body weight in F1 male mice administered a standard diet (STD) or a high-fat diet (HFD). (a) Body weight in offspring administered an STD (left) and an HFD (Braun et al.), (b) The ratio of gWAT mass to body weight in offspring administered an STD (left) and an HFD (Braun et al.). Values represent the mean  $\pm$  SD for each group. The least-squares (LS) means of the phenotypes significantly increased from 5 mg/kg/d ( $p = 0.0036$  for BW,  $p = 0.0018$  for gWAT/BW) in the HFD group, as revealed through the *a priori* contrast test. LS-means with the same letter are not significantly different. No letters in the subpanel imply the absence of treatment effects of BPS.

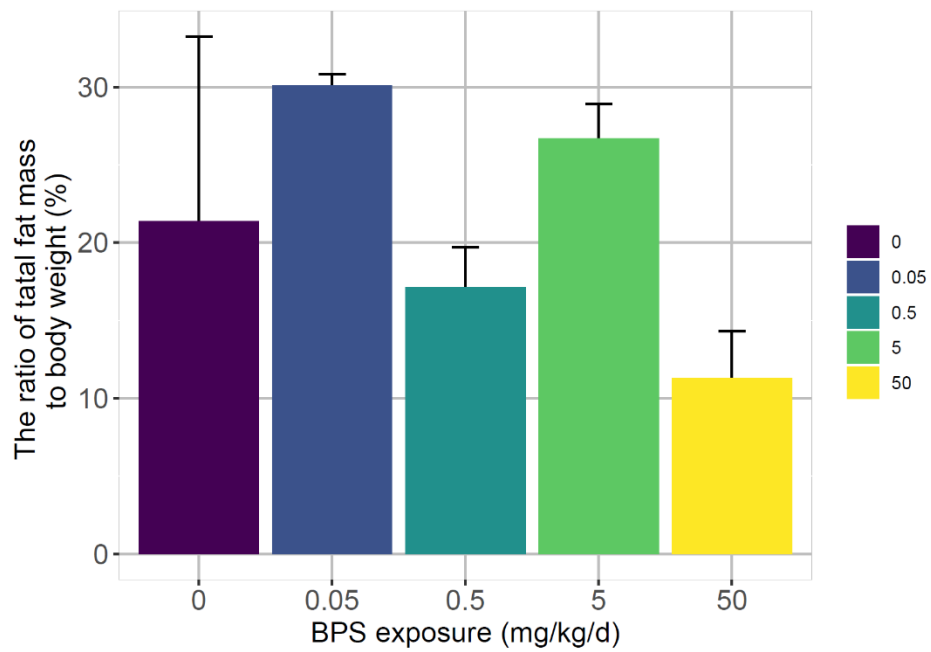


Figure 3-3. The ratios of fat mass to body weight (%) of the offspring ( $n = 15$ ) administered a high-fat diet. Values represent the mean  $\pm$  SD for each group.

### **3.3.2. Food intake and energy expenditure**

The 48-h food intake assay revealed low values at 0.05 mg/kg/d and high values at 50 mg/kg/d groups among the other groups; however, the former was not significantly different ( $p > 0.05$ ), and the latter seemed influenced by an outlier with wide variation. No significant differences were observed in food intake amounts and energy expenditure between the BPS-exposed mice on an HFD and the vehicle-treated control mice (Figure 3-4).

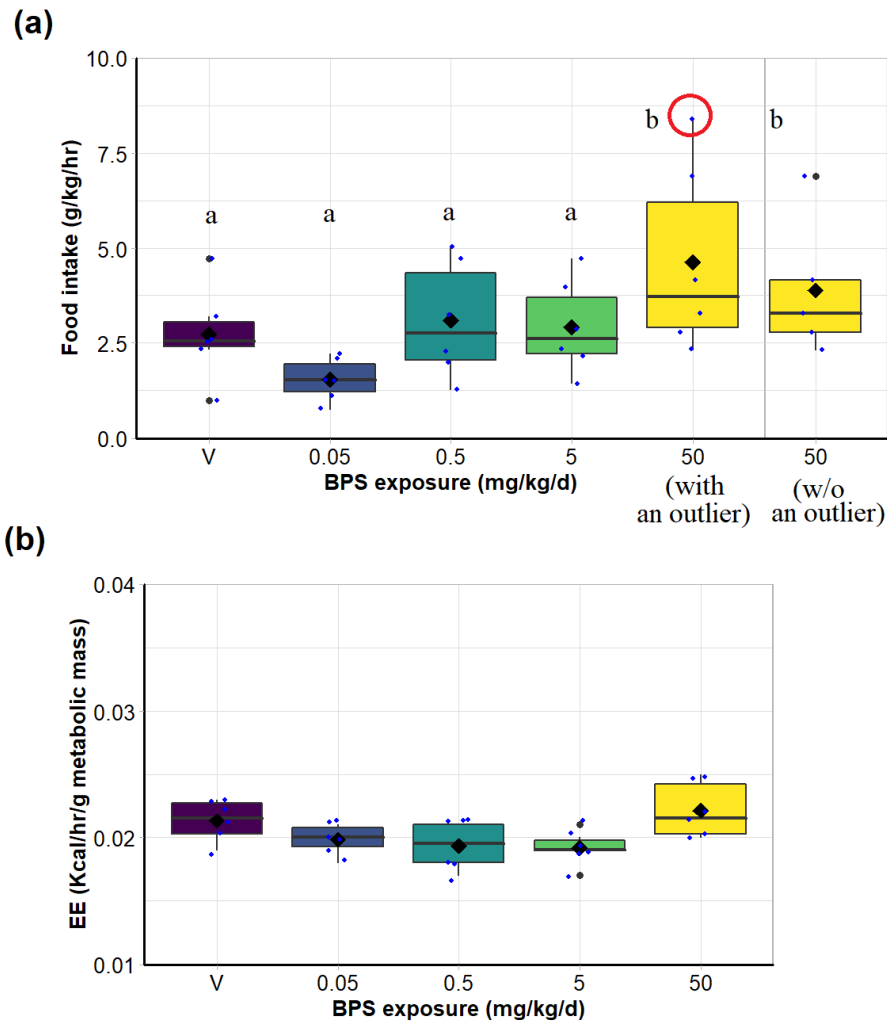
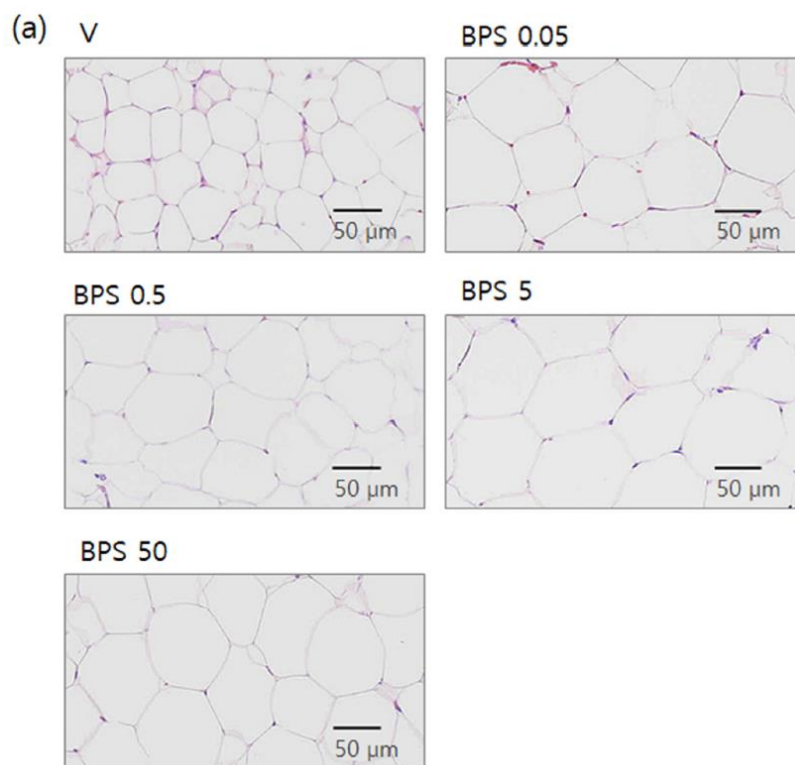


Figure 3-4. Food intake and energy expenditure among offspring ( $n = 15$ ) administered a high-fat diet. (a) Food intake during the day and night in three male mice by group, (b) energy expenditure (EE) in six male mice by group. Representative data on EE were normalized to the metabolic mass (lean mass + 0.2 fat mass) (Even and Nadkarni 2012). LS-means with the same letter are not significantly different on an *a priori* contrast test. Values represent the mean  $\pm$  SD for each group. No letters in the subpanel implies the absence of treatment effects of bisphenol S.

### 3.3.3. Adipocyte hypertrophy in the gWAT

To explore the increases in the gWAT fat mass/BW ratio at various doses of BPS exposure in male mice on a HFD (BPS/HFD), we compared the adipocyte size of the gWAT through histological examination. Adipocytes of the gWAT in the BPS-exposed mice at levels as low as 0.05 mg/kg/d appeared hypertrophied relative to the vehicle-treated control mice on a high-fat challenge (Figure 3-5a), consistent with the *a priori* contrast tests: linearity with dose ( $p < 0.0001$ ) and step-increase trends at 0.05 mg/kg/d and 5 mg/kg/d ( $p < 0.001$ ) for both adipocyte area and diameter (Figure 3-5b, 3-5c).



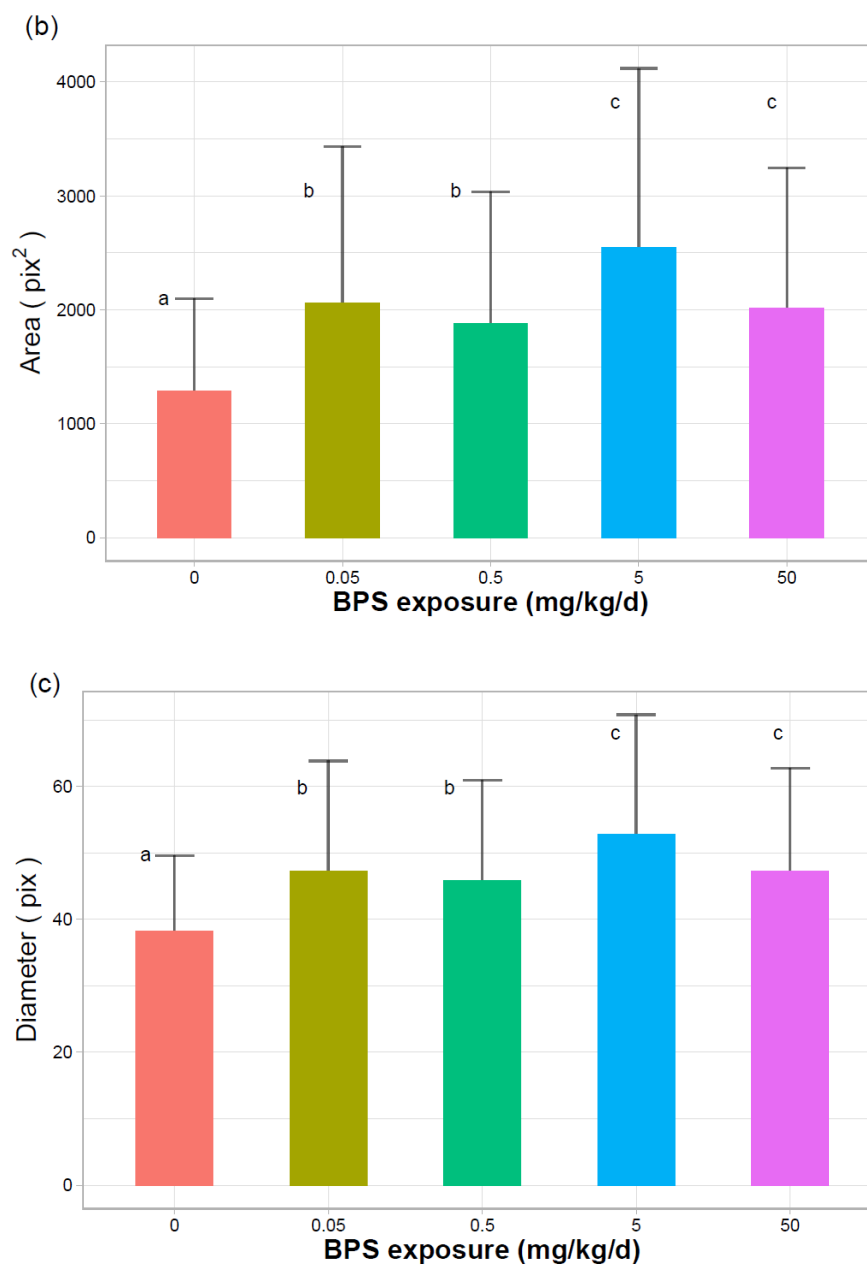


Figure 3-5. Effect of prenatal exposure to bisphenol S (BPS) on adipocyte hypertrophy in the gonadal white adipose tissue (gWAT) in F1 male mice

administered a high-fat diet (HFD). (a) Representative images (magnification, 100×) of hematoxylin-eosin-stained gWAT sections of 3 mice per exposure group, 3 sections per mouse, and 3 fields per section, (b) Adipocyte area from gWATs in each group ( $n = 45$ ), (c) Adipocyte diameter from gWATs in each group ( $n = 45$ ). Values represent the mean  $\pm$  SD for each group.

#### 3.3.4. mRNA expression of adipogenic marker genes

Upregulation of *Pparg* and its downstream markers displayed significant linearity with the dose level ( $p < 0.005$ ) upon multiple comparisons; however, these patterns were not reproduced in STD-fed mice. mRNA upregulation was prominent from 5 mg/kg/d [*Pparg* 2.0-fold ( $p = 0.0010$ ), *Lpl* 2.1-fold ( $p = 0.005$ ) and *Adipoq* 1.3-fold ( $p = 0.0039$ )] and 50 mg/kg/d [*Cebpa* 3.5-fold ( $p = 0.0001$ ) and *Fabp4* 2.8-fold ( $p = 0.0002$ )] (Figure 3-6). Interestingly, slight but non-significant gene downregulation was observed at 0.05 mg/kg [*Cebpa* 0.8-fold; *Fabp4* 0.7-fold; *Lpl* 0.6-fold; *Adipoq* 0.5-fold], 0.5 mg/kg [*Pparg* 0.7-fold; *Lpl* 0.8-fold; *Adipoq* 0.7-fold] and 5 mg/kg [*Cebpa* 0.8-fold].



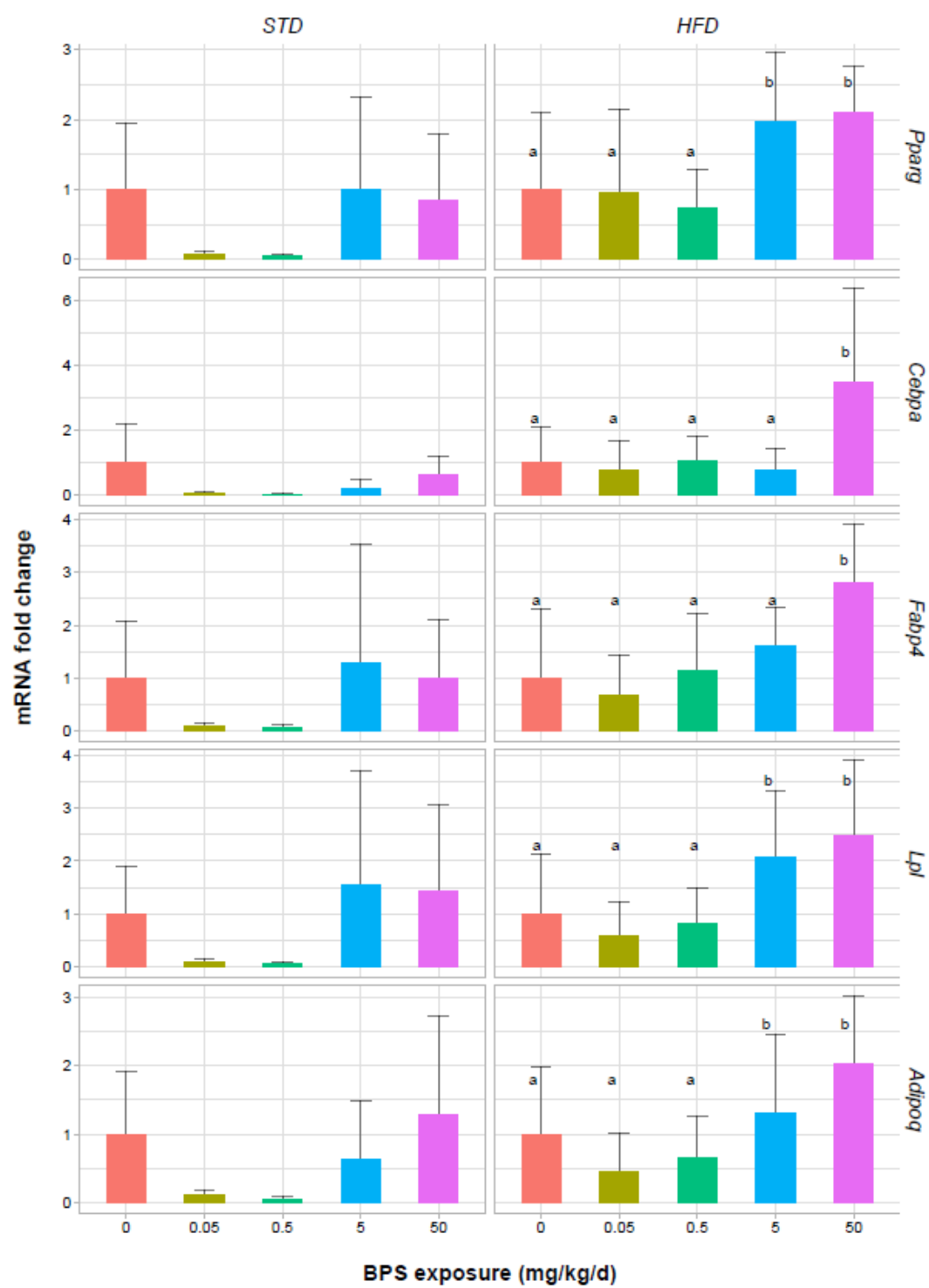


Figure 3-6. Least-squares (LS) means of relative mRNA expression of *Pparg* and its direct target genes in the gonadal white adipose tissue (gWAT) in F1 male mice prenatally-exposed to bisphenol S and those exposed to the vehicle control. STD - standard diet, HFD - high-fat diet. Each value represents the fold-change of relative mRNA expression levels to the average of each vehicle group (mean  $\pm$  SD). mRNA upregulation was prominent from 5 mg/kg/d [*Pparg* ( $p = 0.0010$ ), *Lpl* ( $p = 0.005$ ) and *Adipoq* ( $p = 0.0039$ )] and 50 mg/kg/d [*Cebpa* ( $p = 0.0001$ ) and *Fabp4* ( $p = 0.0002$ )] on *a priori* contrast tests. LS-means with the same letter are not significantly different. No letters in the subpanel imply the absence of the effects of BPS.

### **3.4. Discussion**

#### **3.4.1. Body weight and gWAT changes after prenatal exposure to BPS under HFD-challenge at adult F1 mice**

Although prenatal BPS exposure did not drastically alter the body weight and the gWAT mass, adult F1 mice had a high adipogenic predisposition at BPS levels as low as 5 mg/kg/d; however, this was only observed at a high-fat challenge. Furthermore, marked variations in body weight and gWAT mass were observed (Figure 3-2, Table 3-4), suggesting interindividual variations among F1 mice after a high-fat challenge for 4 weeks, which was relatively shorter than those in the conventional obesity assay (e.g.,  $\geq 12$  weeks), concurrent with a previous report (Podrini et al. 2013). Histological analyses of BPS-exposed groups revealed enlarged gonadal adipocytes compared to the control mice (Figure 3-5), consistent with our speculation that prenatal exposure to BPS influences the susceptibility to HFD-induced adipogenesis.

Table 3-4. Coefficient of variations for body weight and the relative mass of gonadal white adipose tissue to the body weight

		STD			HFD		
Phenotypes	Group	<i>n</i>	Mean	CV(%)	<i>n</i>	Mean	CV(%)
Body weight (g)	Control	13	24.2	2.63	16	28.6	13.9
	BPS <sup>a</sup>	41	23.3	10.7	28	30.2	11.9
	0.05	6	25.5	1.98	6	28.2	5.92
	0.5	3	22.2	1.81	4	27.3	21.4
	5.	13	22.8	15.6	8	32.4	29.64
	50.	19	23.2	7.88	10	30.9	8.76
gWAT/BW (%)	Control	13	1.61	25.2	16	3.93	48.2
	BPS <sup>a</sup>	41	1.63	27.7	28	4.54	35.7
	0.05	6	1.82	28.4	6	3.20	33.3
	0.5	3	1.47	23.5	4	3.32	48.6
	5.	13	1.46	24.2	8	5.18	28.4
	50.	19	1.72	28.4	10	5.31	25.1

<sup>a</sup> BPS 0.05, 0.5, 5 and 50 mg/kg/d groups.

Based on a previous report wherein fat mass increased in male offspring upon BPS exposure, (*perinatal* exposure to BPS and HFD for 22 weeks after weaning), we focused on male mice (Ivry Del Moral et al. 2016); however, that study did not clarify when the critical change in susceptibility occurred in terms of the exposure window of BPS, and whether BPS functioned as an adipogenic agent *per se* or as stimulator among subjects more prone to adipogenesis. Considering the similarity of the chemical structure of BPS and BPA and recent reports (Ahmed and Atlas 2016; Boucher et al. 2016a; Pu et al. 2017), we cannot exclude the possibility that BPS could be involved in the mammal adipogenesis, as opposed to BPA (Garcia-Arevalo et al. 2014; Vom Saal et al. 2012). Our findings suggest that BPS exposure potentially exacerbates HFD-induced adipogenesis and presents a critical window of susceptibility by exposing pregnant mice to BPS for the second half of the gestation period. To our knowledge, our study is the first to reveal the male-specific adipogenic effects of a prenatal exposure (9 d in utero) to BPS in F1 adults.

Extensive evidence indicates that EDCs play a role in reprogramming obesity-prone phenotypes (Janesick and Blumberg 2011; Lin et al. 2017; Vom Saal et al. 2012). Herein, no significant differences in body weights at postnatal day 1 were observed between the BPS-exposed and control groups, concurrent with a previous report on fetal sheep models of perinatal BPS exposure (Pu et al. 2017); moreover, these trends in body weight were maintained until 6 weeks before the HFD challenge (data not shown), potentially suggesting that prenatal BPS exposure

does not influence birth weight or early life stages herein.

### 3.4.2. Upregulation of adipogenesis-related transcription in the gWAT

Consistent with the enlarged gonadal adipocytes observed upon histological analysis among the BPS-exposed groups (Figure 3), comparable activation of adipogenic gene expression was observed in the gWAT in F1 male mice (Figure 4). We assumed that BPS-mediated transcriptional modulation was induced in a dose-dependent manner (Ahmed and Atlas 2016), and that the adipogenic effects of BPS treatment could be induced upon a high-fat challenge (Wei et al. 2011). Presumably, prenatal BPS exposure could stimulate the overexpression of mRNAs for *Pparg* and its direct target genes, *Cebpa*, *Fabp4*, *Lpl* and *Adipoq* in HFD-fed male mice. It is well established that PPAR $\gamma$  is a master transcriptional regulator of adipogenesis that is co-regulated with another key transcription factor C/EBP $\alpha$ , and both are involved in adipogenesis (Gregoire et al. 1998). Moreover, these factors could be upregulated through prenatal BPA exposure as well (Somm et al. 2009). Thus, it is reasonable to assume that BPS potentially upregulates *Pparg* and its downstream targets.

Numerous EDCs stimulate adipogenesis by stimulating either adipocyte maturation or differentiation into adipocytes. PPAR $\gamma$  could probably serve as a primary target (Regnier and Sargis 2014), as reported in some recent *in vitro* studies on BPS (Ahmed and Atlas 2016; Boucher et al. 2016a). Another *in vitro* study reported that PPAR $\gamma$  and LEP were upregulated after adipogenic differentiation in

swine adipose stromal cells (Berni et al. 2019). Concurrent with these results, our results indicate that prenatal BPS exposure potentially upregulates *Pparg* and its downstream targets (Figure. 4).

Herein, *Pparg* mRNA was upregulated upon prenatal BPS exposure before administering an HFD (BPS/HFD), but not in the BPS/STD group. BPS may probably serve as a PPAR $\gamma$  agonist. Thus, the modestly active conformation of PPAR $\gamma$  could be achieved through a complex with BPS, then facilitating direct interaction of natural ligands in HFD to adopt a completely active PPAR $\gamma$  conformation for adipocyte differentiation. A previous *in vitro* study reported that *Pparg2* and *aP2* (adipocyte lipid binding gene, aka *Fabp4*) expression levels remained unchanged on BPS exposure, PPAR $\gamma$  coactivator  $\alpha$  (PGC-1 $\alpha$ ) was upregulated upon BPS exposure in murine 3T3-L1 cells (Helies-Toussaint et al. 2014), and BPS activated PPAR $\gamma$  expression, thus promoting lipid droplet formation in murine 3T3-L1 cells (Ahmed and Atlas 2016). Although further mechanistic studies are required for explicit validation, it is plausible that the synergetic inclination towards adipogenicity might occur upon prenatal BPS exposure followed by delayed-HFD in adult male mice.

Furthermore, herein, *Cebpa* was also markedly upregulated, since it is a direct target of the master regulator *Pparg*. In a rat study on perinatal BPA exposure, the treatment group displayed numerous upregulated genes in abdominal adipocytes in adults, including *Cebpa*, *Pparg*, and *Lpl* (Somm et al., 2009). In



humans, *CEBPA* mRNA levels in adipocyte tissue were higher in those with an obese phenotype than in those with a lean phenotype (Krempler et al., 2000). PPAR $\gamma$ , expressed in adult adipocytes, and C/EBP $\alpha$  are both regulators of lipogenesis, and PPAR $\gamma$  activation results in increased fat deposition (Gregoire et al., 1998; Yamauchi et al., 2001; Zhang et al., 2004).

*Adipoq* (encoding adiponectin) upregulation during adulthood after an HFD challenge (Figure 4) may reflect certain changes associated with *Adipoq* (or related with upstream-genes) *in utero*. Although we did not assess *Adipoq* mRNA levels in fetal preadipocytes, the present results indicate that BPS-induced *Adipoq* expression at 10 weeks may have resulted from certain alterations *in utero*. Ivry Del Moral et al. (2016) reported that long-term exposure (gestation + 22 weeks) to a low dose (up to 0.05 mg/kg/d) of BPS with an HFD downregulated *Pparg* and *Adipoq*, concurrent with the present results. However, it remains unclear whether this upregulation follows a monotonous trend, and hence further studies are required to confirm this point. In contrast, Pu and Veiga-Lopez (2017) assessed fetal and adult ovine preadipocytes requiring a PPAR $\gamma$  agonist at the terminal adipogenic differentiation phase, and their results are concurrent with the present results (Pu and Veiga-Lopez 2017). Analyses of transcription profiles in differentiating human primary preadipocytes treated with BPS or BPA revealed that *ADIPOQ* was upregulated in BPS-treated preadipocytes but not in BPA-treated preadipocytes. Considering further evidence regarding preadipocyte differentiation upon BPA and

BPS exposure in human tissues, BPS could be much more efficient than BPA for elevating adipogenic regulators (Boucher et al. 2016b).

Furthermore, our results indicate that *Lpl* (encoding lipoprotein lipase) upregulation may help maintain triglyceride levels in male offspring upon prenatal BPS exposure, which could not be analyzed herein, since TG levels were not measured in the adipose tissue or the liver. In general, LPL is synthesized in adipose tissues and then secreted and attached to the endothelium of the adjacent blood capillaries, where it hydrolyzes TG, contained in chylomicrons and very-low-density lipoproteins, to fatty acids. Furthermore, *LPL* is regulated by estrogens (Misso et al. 2003). In mouse 3T3-L1 cells, BPA increased LPL activity and triacylglycerol accumulation and led to the generation of larger lipid droplets in the differentiated cells (Masuno et al., 2002).

There are some limitations regarding the study design and methods herein. First, the timing of euthanasia of the mice differed depending on the diet type. Moreover, this study combines two separate experiments based on the study objectives, albeit independently conducted. Both experiments investigated the adipogenic effect of prenatal BPS exposure in adult F1 mice. The experiment with STD lasted up to 8 weeks with no significant change in phenotype, whereas the second independent experiment involving a high-fat challenge displayed a minor phenotypic change. Obesity can be induced through an HFD for >4 weeks (Donovan et al. 2009; Podrini et al. 2013) after 6 weeks of age when mice reach

sexual maturity. To fulfil the criteria for euthanasia, the HFD should have been administered to 4-week-old mice or those administered an HFD for periods shorter than 4 weeks. Nonetheless, each diet type included both BPS-treated and vehicle control groups, and the primary purpose of this study was to monitor the consequent adipogenesis depending on BPS exposure (Figure 1).

Second, this study only involved male mice, based on previous studies on perinatal exposure to BPS and obesity having reported associations among male mice and sheep (Ivry Del Moral et al. 2016; Meng et al. 2018; Pu et al. 2017). Our results confirm the effect of prenatal BPS exposure with histological images and adipogenesis marker expression. Although a comparison was not made with female mice herein, it does not nullify the results obtained with male mice. Further studies are required to investigate sex-dependent adipogenic effects of BPS exposure.

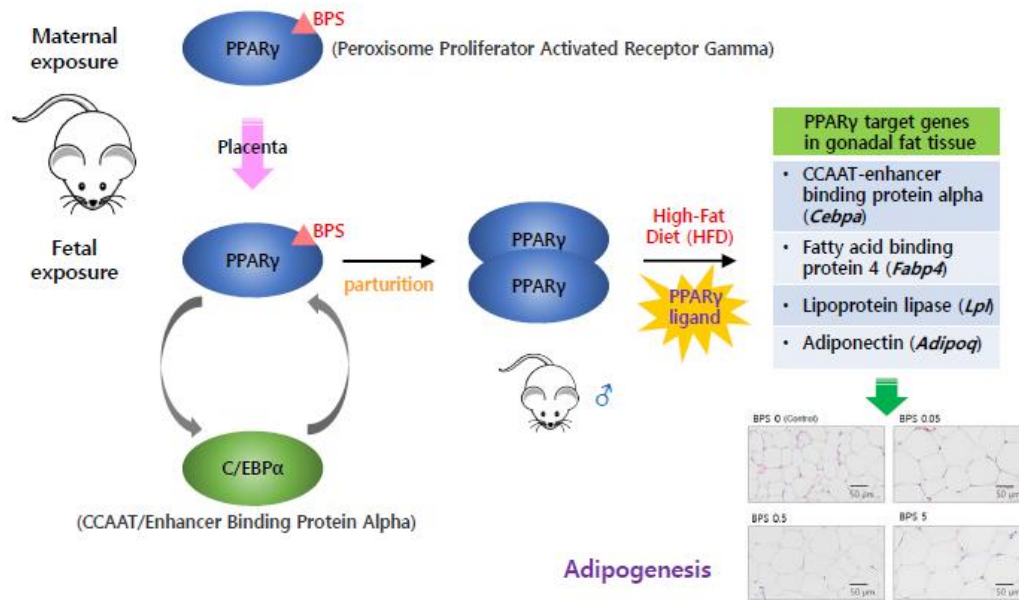
The third limitation is regarding the exposure window for BPS during gestation. The pregnant dams herein were imported at GD2; thereafter, they were exposed to BPS through drinking water from GD9 to parturition. This period corresponds to fetal programming leading to adipocyte development in mice. Concurrently, environmentally induced molecular modulation may occur in somatic cells immediately after global DNA demethylation, while the erasure of parental DNA methylation has just been initiated in the germline cells (Faulk and Dolinoy 2011; Gluckman et al. 2009). This is one of the most sensitive periods wherein prenatal environmental factors alter fetal gene expression patterns against the health

status for subsequent generations (Martin and Fry 2018). Therefore, the BPS exposure window herein potentially represents an epigenetically vital stage, although changes in DNA methylation cannot account for all diseases resulting from environmental factors.

Finally, some study limitations were associated with the dose-response and the associated underlying mechanism. Although a linear tendency in phenotypic changes and upregulation of adipogenesis markers were observed upon exposure of 0.05–50 mg/kg/d of BPS, we could not determine the extent of the effect of minimum doses of prenatal BPS exposure. Furthermore, adipocyte hypertrophy was observed at lower BPS doses than those resulting in the upregulation of *Pparg* and its target genes. These markers reportedly facilitate the differentiation of pre-adipocytes to mature adipocytes; however, they might not play a crucial role in adipocyte enlargement. Further studies are required to address this aspect.

Despite the aforementioned limitations, this study provides evidence of F1-specific changes in the gWAT and the concordant upregulation of adipogenesis regulators in male mice exposed prenatally to BPS. The present results suggest that *in utero* BPS exposure increases the predisposition for adipogenesis among male fetuses, which could manifest after adulthood, especially upon high-fat insult. Further studies are required to determine whether BPS is causally associated with epigenetic modifications as a prerequisite for fetal adipogenic programming.

## Graphical summary



## Chapter 4. **BPS-responsive DNA methylation of *Igf2* in adult F1 male mice**

### **4.1. Introduction**

Exposure to obesogenic EDCs such as BPA in utero environment is speculated to lead to programmed changes during fetal development, and epigenetic processes including DNA methylation are thought to play an important role (Egusquiza and Blumberg 2020; Stel and Legler 2015; Tudurí et al. 2018). DNA methylation, the addition of a methyl group to the cytosine residue of DNA is most studied mechanism of epigenetic dysregulation that environmental chemicals can alter gene expression and lead to adult-onset diseases (Lane 2014; Saffery and Novakovic 2014).

IGF2 has a growth promoting effect, and *IGF2/H19* locus is involved in fetal programming through DNA methylation to control growth and body composition (Constância et al. 2002; Huang et al. 2012). The *IGF2* gene and adjacent *H19* non-coding RNA are clustered in an imprinted region on chromosome 11 in humans and chromosome 7 in mouse (Sasaki et al. 2000). Most imprinted genes exist in clusters. The cluster is regulated by an ICR on the maternal and paternal alleles. These allele-specific methylation imprints are established in germ cells and, after fertilization,

they are maintained during embryonic development and in somatic tissues.

It has been known that developmental and antenatal period outlines as a sensitive and critical window of vulnerability because early-life exposure to BPA and other chemicals can epigenetically program the adult-onset obesity and metabolic diseases (Stel and Legler 2015; Tudurí et al. 2018; Zhu et al. 2019). For example, it is found that prenatal exposure to BPA can alter the epigenetic signature of cells and tissues leading to a disease phenotype (Stel and Legler 2015). Another research team reported that continuous maternal exposure to BPA during oocyte maturation affected DNA methylation of ICR in *Igf2/H19* domain (Susiarjo et al. 2013). An *in vitro* study has been demonstrating decreased global DNA methylation in 3T3-L1 cell line (Bastos Sales et al. 2013). However, information on BPS-induced epigenetic changes on adipose tissue is still limited.

This study was designed to cover the development of adipose tissue of F1 mice through the maternal exposure to BPS. So far, it was found in chapter 3 that prenatal exposure to BPS could affect fat mass in adulthood. Considering the exposure period and adipogenic effects in the previous results, it is necessary to examine whether there are BPS-induced epigenetic changes in adult adipose tissue.

The purpose of the study in this chapter is to explain that BPS can affect epigenetic modifications during adipocyte differentiation and the development of adipose tissue. The hypothesis here is that prenatal exposure to BPS will affect the DNA methylation of *Igf2*, the imprinting gene related to adiposity. To prove this

experimentally, changes in DNA methylation of *Igf2/H19* ICR were observed using adult adipose tissue of F1 males.



## **4.2. Materials and methods**

### **4.2.1. DNA isolation and bisulfite conversion**

- **gWAT samples and genomic DNA**

Each gWAT of male mice was cut on the iced plate and weighed up to 25 mg for genomic DNA isolation. Sample size in STD group; n=13 (0 mg/kg/d), n=6 (0.05 mg/kg/d), n=3 (0.5 mg/kg/d), n=13 (5 mg/kg/d), n=19 (50 mg/kg/d). Sample size in HFD group; n=16 (0 mg/kg/d), n=7 (0.05 mg/kg/d), n=4 (0.5 mg/kg/d), n=8 (5 mg/kg/d), n=10 (50 mg/kg/d).

The gWAT cuts were purified for genomic DNA using the spin column protocol of DNeasy Blood & Tissue kit (Cat. 69506, QIAGEN, Hilden, Germany) according to the manufacturer's instructions. The purified genomic DNA was qualified and quantified using the Nano Drop spectrophotometer, and stored at -80 until next step.

- **Bisulfite converted genomic DNA**

200 ng of the DNA was bisulfite treated using EZ DNA Methylation-Lightning Kit (D5050, Zymo Research, South Korea)

following manufacturer's protocol.

#### 4.2.2. PCR amplifications and Pyrosequencing analysis

- Biotinylated PCR product

One microliter of the bisulfite converted DNA was mixed with 24  $\mu$ L of the reaction cocktail containing HS Prime Taq DNA Polymerase (G-7000, GENETBIO, South Korea) and the primers of H19/Igf2 ICR according to the manufacturer's instruction. The primer sequences for H19/Igf2 ICR were as follows: forward primer 5'-GGGTAGGATATATGTATTTTTTAGGTTG-3' and biotinylated reverse primer 5'- CTCATAAAACCCATAACTATAAAATCAT-3'. The amplicon size is 221 bp. And then, PCR amplifications were performed in PTC-200 thermal cycler (MJ Research, Watertown, MA) and the conditions were: 96 °C for 5 minutes (initial denaturation) followed by 50 cycles of 95 °C for 30 seconds (denaturation), 52°C for 30 seconds (annealing), 72 °C for a minute (extension), 72 °C for 10 minutes (final extension), and 4 °C for an extended cooling period. At least two independent PCRs were performed on each sample.

The biotinylated PCR products (3  $\mu$ L) were separated by

electrophoresis in 1.5 % agarose gels in 0.5x TAE buffer containing RedSafe™ Nucleic Acid Staining Solution (Cat. 21141, iNtRON Biotechnology, South Korea). The DNA fragments were visualized under UV light and captured the photos using the software. The molecular weights of the amplification products were confirmed with 1-kb DNA ladder standards. The remaining biotinylated PCR product (about 20 µL) was used for replicate pyrosequencing runs.

- Pyrosequencing analysis

Pyrosequencing was conducted on a PyroMark Q48 Autoprep instrument (QIAGEN, CA) using the PyroMark Q48 Advanced CpG Reagents (QIAGEN, CA) and the H19/Igf2 ICR sequencing primer 5'- TGTAAGATTAGGGTTGT- 3' according to the manufacturer's instructions. Percent methylation (%) was assessed across six CpG sites at imprinting control region (ICR) for *Igf2/H19* (adapted from Susiarjo 2013). The percentage of DNA methylation was calculated with the PyroMark Q48 Autoprep 2.4.2 software (QIAGEN, CA).

#### 4.2.3. Statistical Analysis

Data were collected from experiment duplicates. *Igf2* ICR-specific methylation levels were analyzed by a non-parametric test. To evaluate the statistical differences in the percentage of DNA methylation among exposure groups, Kruskal-Wallis test was performed using R.

### **4.3. Results**

To test the hypothesis, we treated pregnant mice starting from GD9 to GD18 (PND 0 of F1 mice). with three different doses of dietary BPS: 0 (control), 0.05, 0.5, 5, and 50 mg/kg/d. DNA methylation of *Igf2/H19* ICR was observed in gWAT of F1 male mice in adulthood.

#### **4.3.1. DNA methylation of *H19/Igf2* ICR in gWAT**

The overall percent (%) of DNA methylation in *Igf2/H19* in gWAT represented in Figure 4-1. Without distinguishing each CpG site, the levels of DNA methylation were not BPS-dependent, statistically.

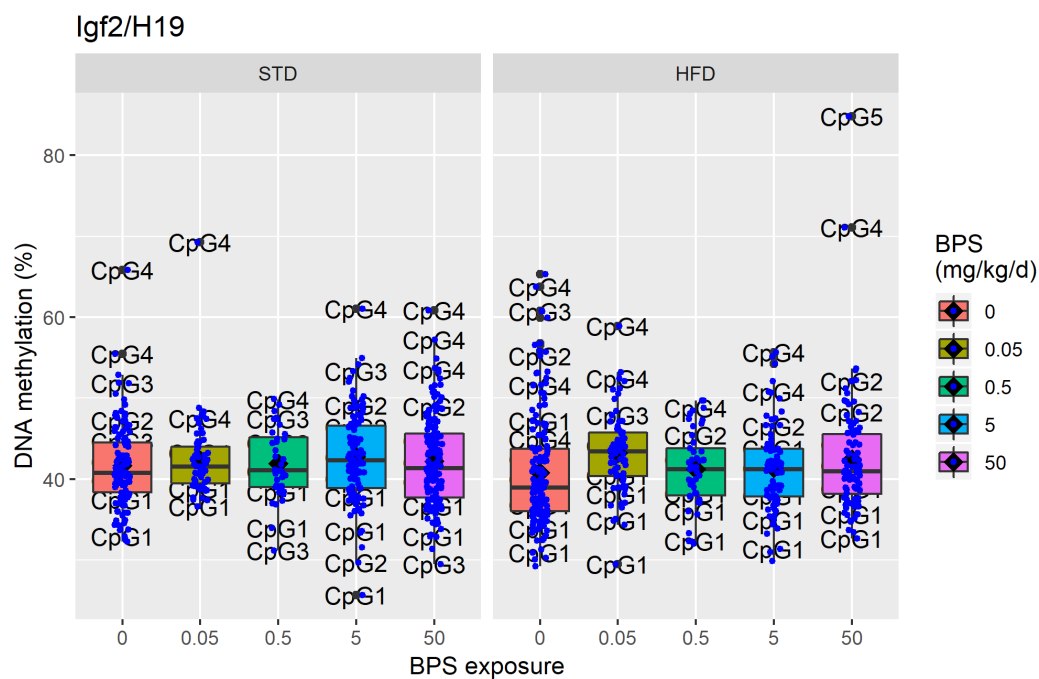
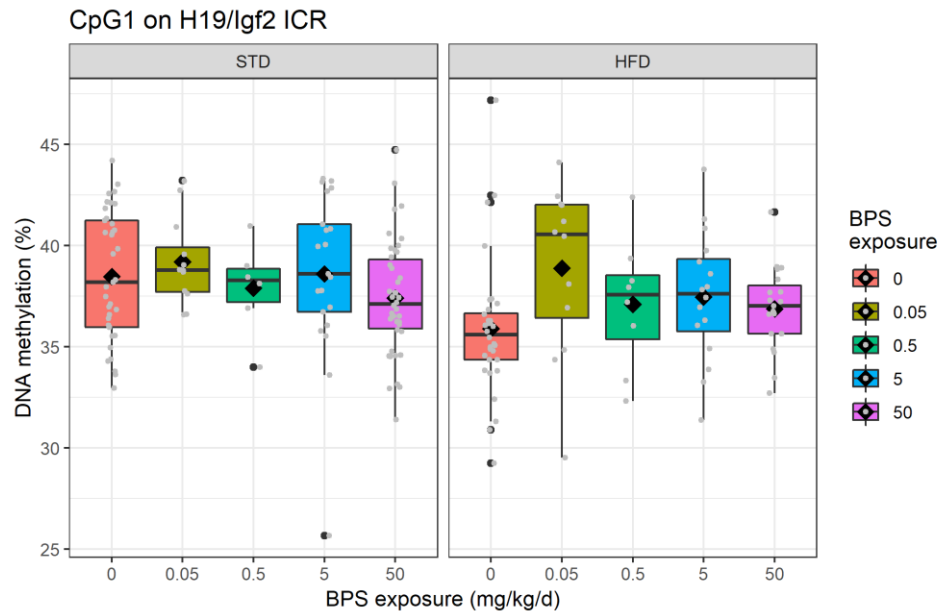


Figure 4-1. The overall level of DNA methylation on *Igf2/H19* ICR in gonadal adipose tissues of F1 male mice prenatally exposed to BPS. STD; standard diet, HFD; high-fat diet.

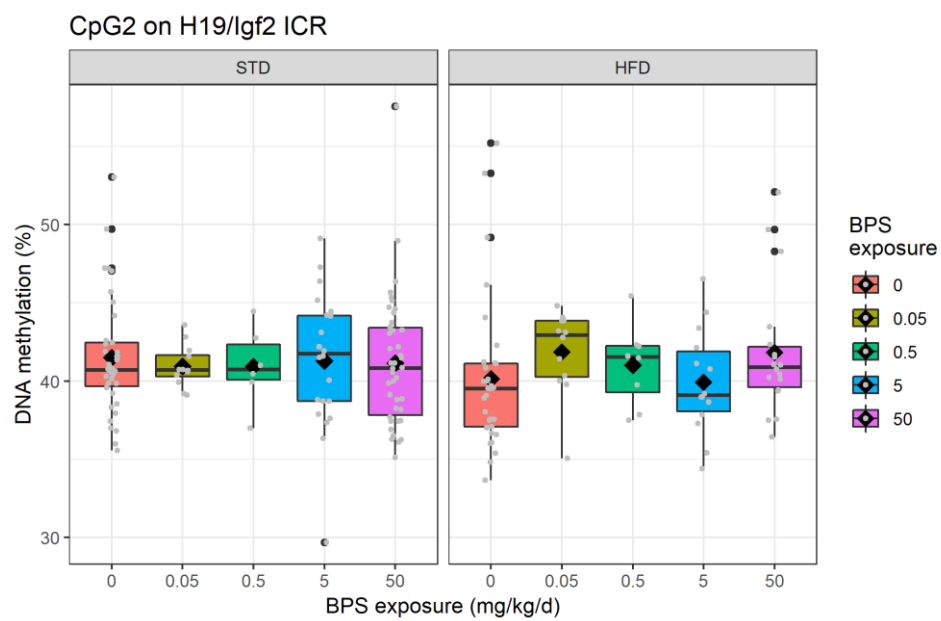
#### 4.3.2. BPS-related CpG sites on *Igf2/H19* in gWAT

BPS-related CpG sites in *Igf2/H19* were shown in Figure 4-2. The CpG1 showed significantly different DNA methylation levels among BPS groups in male mice fed with HFD ( $p < 0.05$ ), but not with STD ( $p = 0.17$ ). The CpG2 did not show significantly different DNA methylation levels among BPS groups in male mice fed with STD ( $p > 0.05$ ) and HFD ( $p > 0.05$ ). The CpG3 showed significantly different DNA methylation levels among BPS groups in male mice fed with HFD ( $p < 0.05$ ), but not with STD ( $p = 0.9$ ). The CpG4, CpG5 and CpG6 did not show significantly different DNA methylation levels among BPS groups in male mice fed with HFD ( $p > 0.05$ ) and STD ( $p > 0.05$ ).

(a)

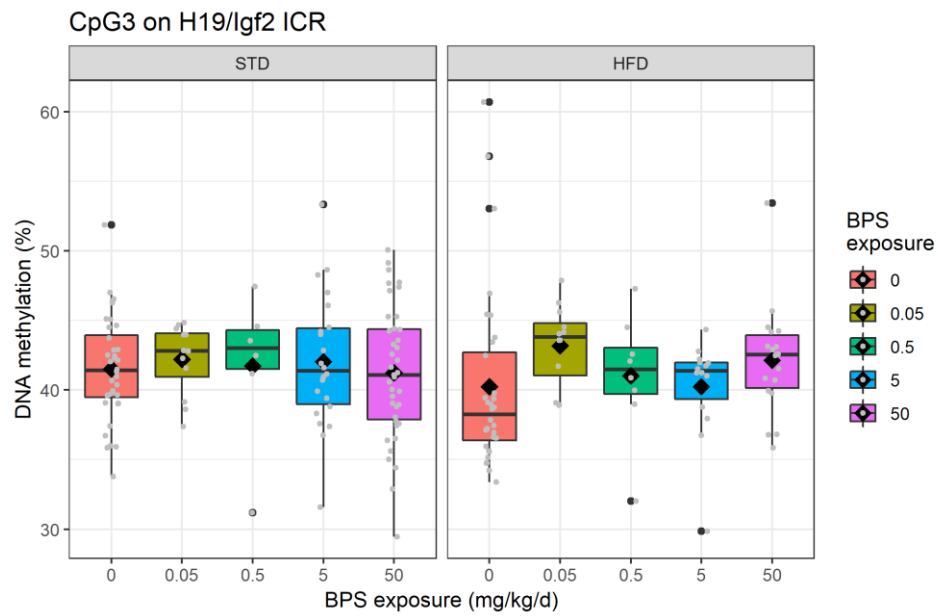


(b)

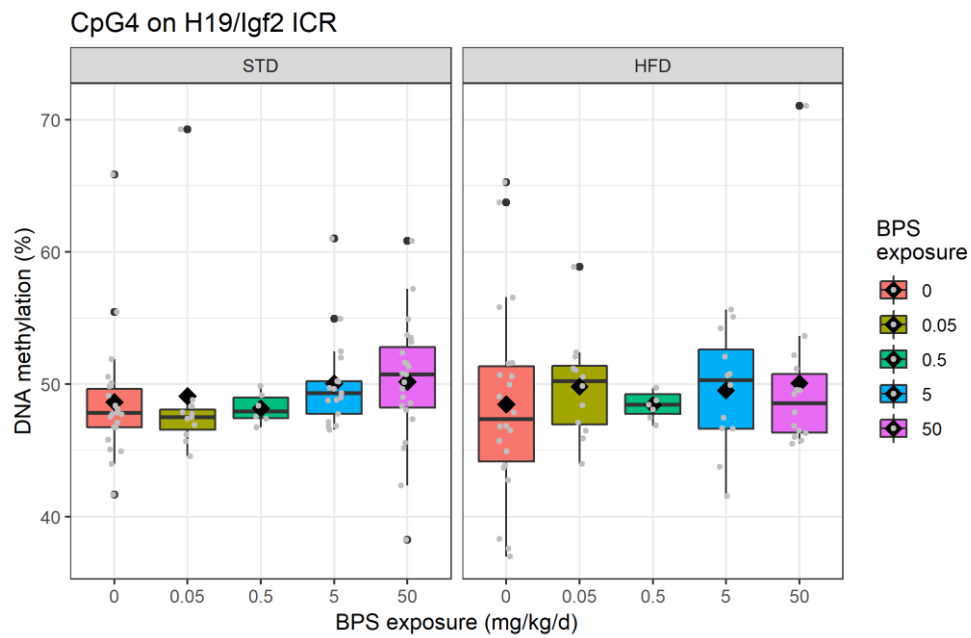




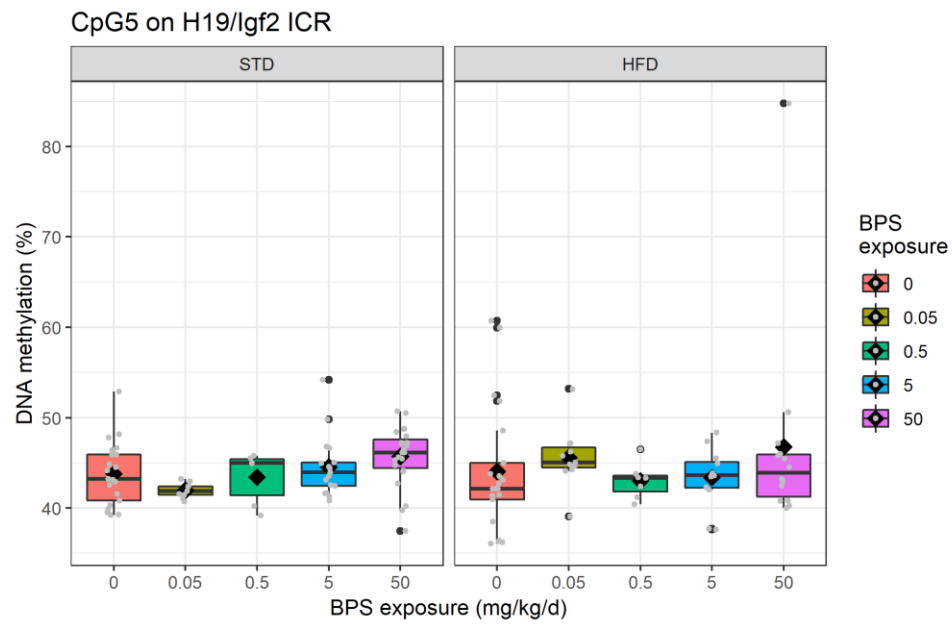
(c)



(d)



(e)



(f)

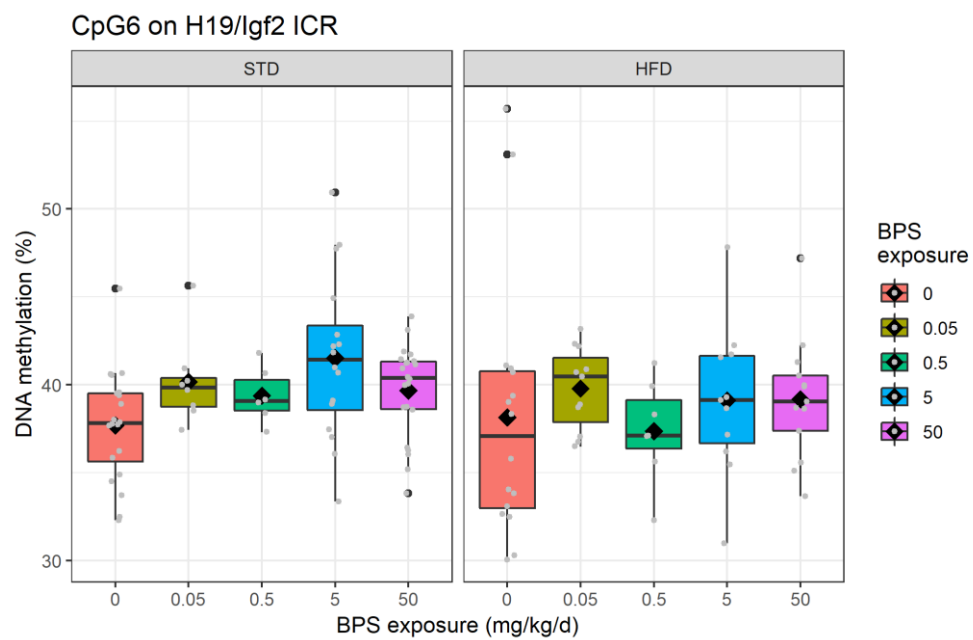


Figure 4-2. The levels of DNA methylation at six CpG sites on *Igf2/H19* ICR in gonadal adipose tissues of F1 male mice prenatally exposed to BPS. (a) DNA methylation at CpG1 on *Igf2/H19* ICR. (b) DNA methylation at CpG2 on *Igf2/H19* ICR. (c) DNA methylation at CpG3 on *Igf2/H19* ICR. (d) DNA methylation at CpG4 on *Igf2/H19* ICR. (e) DNA methylation at CpG5 on *Igf2/H19* ICR. (f) DNA methylation at CpG6 on *Igf2/H19* ICR. The black diamonds in the boxplots represent the mean values and the grey dots represent the individual sample data.

#### 4.4. Discussion

Environmental obesogens can increase the susceptibility to obesity across generations through epigenetic transgenerational inheritance (Bansal et al. 2019; Schug et al. 2011; Zhang et al. 2019). In the current study, the F0 maternal mice were exposed to BPS during the critical period of fetal development when PGCs proliferate to form germ cells as well as adipocytes differentiate and proliferate to form adipose tissues. Previous chapters showed an increased susceptibility to adiposity in F1 generation maternally exposed to BPS. This chapter investigated whether there were changes in DNA methylation of *Igf2/H19* ICR in gWAT according to the dose of BPS. It didn't appear that there were significant changes in the overall percentage of DNA methylation from the six CpGs tested (Figure 4-1). Interestingly, in additional analysis with the individual CpG site, some BPS-responsive CpG sites of *Igf2/H19* ICR were observed (Figure 4-2). Collectively, these results suggested that BPS has the potential to affect specific CpG sites of *Igf2* involved the processes of growth and fat mass, and thus an increased propensity for adiposity.

In some cases of obesogenic EDCs, maternal exposure to BPA has been observed in mice to disrupt DNA methylation at some ICRs (imprinting control regions). BPA-induced DNA methylation has been linked to improper expression of imprinted genes related development in embryos and placenta. Importantly, that

was linked to abnormal development in the F1 placenta. When maternal exposure to BPA occurs especially before mating, BPA affected increased DNA methylation at the *Igf2* DMR and *Snrpn* ICR and increased expression of the growth factor at embryonic day 9.5 and 12.5 (Susiarjo et al. 2013).

One of the most interesting finding of the present study is that BPS exposure (GD9-GD18) covering the period of mid-gestation was correlated with DNA methylation of *Igf2/H19* ICR in gWAT. BPS-related CpG sites existed on *Igf2/H19* domain even though it was not dose-dependent. Unlike the study that BPA exposure from GD5.5 to GD 12.5 did not lead to imprinting defects in embryonic tissues and placenta (Susiarjo et al. 2013), our finding suggested that BPS exposure during mid-gestation can lead to altered DNA methylation of *Igf2/H19* ICR. This outcome appears similar to the other previous studies in that obesogenic effects of EDCs (phthalates, DDTs, tributyltin, etc.) can link to DNA methylation of imprinting genes. It implies that CpG-specific analysis of *Igf2* rather than global methylation are essential in further researches on exposure after fertilization and impl.

Additional finding is that different DNA methylation of certain CpGs site of *Igf2* was observed in lower exposure group as well. BPS-dependent DNA methylation was anticipated in upper exposure group based on the previous chapters. Neonatal BPS retained (Chapter 2) and adipogenic effects in adulthood (Chaper 3) were found in upper exposure groups. BPS metabolites at PND 1 were not

completely excreted out one day after birth in BPS 50mg/kg/d group, and the phenotypic changes in gWAT were clearly observed in BPS 5 and 50 mg/kg/d groups.

Although the current study shed light on the epigenetic changes focusing on BPA-related *Igf2/H19* ICR (Susiarjo et al. 2013) to elucidate whether BPS could affect the similar outcomes of BPA, there are a few limitations.

Limitation of our screening method is that only six CpG sites on *Igf2/H19* ICR were tested. Nevertheless, the current study suggested the levels of DNA methylation may change for certain CpG sites of *Igf2/H19* in response to BPS. And, imprinted expression could not be observed because *Igf2* is abundantly expressed in brain, not in adipose tissues. Since adipose tissues were used as a target tissue for adiposity, DNA methylation in gWAT can be explained as the epigenetic evidence on adipogenic effects. Furthermore, several studies on the effects of BPA on imprinted gene expression (Chao et al. 2012; Doshi et al. 2013; Manikkam et al. 2013; Smith and Taylor 2007; Susiarjo et al. 2013; Zhang et al. 2012) have supported our observation in adult F1 mice. A study on transgenerational effects reported maternal exposure to BPA during mid-gestation (GD 8.5 to 12.5) affected expression of imprinted gene including *Igf2r*, *Rasgrf1*, *Usp29*, *Slc38a4* and *Xist* in embryonic tissues (Kang et al. 2011). It is unclear exactly how the imprinted genes in brain control the processes underlying the morphology of adipose tissue, however, obesogenic chemicals are possibly linked to epigenetic programming directly or

indirectly (Bastos Sales et al. 2013; Drobna et al. 2018; Egusquiza and Blumberg 2020; Saffery and Novakovic 2014; Stel and Legler 2015; Zhang et al. 2019).

## Chapter 5. Overall conclusions

In conclusion, this dissertation contributes to a better understanding of the link between prenatal exposure to BPS and adiposity effects in later life. The effect of in utero exposure to BPS on obesity in later life was determined through a series of three studies. While most *in vivo* studies have not experimentally evaluated residual BPS delivered through pregnant mother to investigate its health effect in next generation, we, in the first part of proceeding, clearly showed that *in utero* BPS can be not only delivered through the mother but also still retained in neonatal body. Most importantly, we supported that *in utero* exposure to BPS can affect manifestation of adiposity by HFD insult as a *Pparg* ligand in adulthood by determining the alteration of adipogenic markers. Also, the present study emphasized the importance of a vulnerable period of exposure to BPS during fetal development to have impacts on susceptibility to adiposity by evaluating DNA methylation of imprinting gene related to obesity. Therefore, the current study filled the knowledge gaps in previous studies and major findings from each study are as follows.

In the first study (Chapter 2), each of the BPS metabolites was determined at postnatal day 1 (PND1) to investigate whether maternally delivered BPS was



totally excreted. By detecting BPS raw materials and metabolites in the PND1 biological sample, it can be confirmed that BPS was transmitted from the mother. The sum of BPS metabolites accounted for 14.6 % of the mother's exposure after 1 day of discontinuation. In the highest exposure group (BPS 50 mg/kg/d), free-BPS, BPS-G, and BPS-S were still detectable one day after birth. BPS-S was predominant, followed by free BPS in neonatal liver, and BPS-G was the most abundant, followed by free-BPS and BPS-S in the rest of body. The amounts of BPS conjugates were more retained in non-liver samples.

In the second study (Chapter 3), fetal BPS-induced changes in adiposity phenotypes and adipogenic marker genes were investigated in adult-staged offspring. With regard to adiposity phenotype, gestational BPS exposure impacted on increases in body weight and gWAT mass of male offspring with a HFD for only 4 weeks, which was relatively shorter than those in the conventional obesity assay. Also, BPS-exposed groups showed enlarged gonadal adipocytes, consistent with our speculation that prenatal exposure to BPS influences the susceptibility to HFD-induced adipogenesis. The key adipogenic marker genes, interestingly, were overexpressed by gestational BPS exposure. These findings imply exposure to BPS during fetal development leads to increased susceptibility for adiposity. The present results suggest that *in utero* BPS exposure increases the predisposition for adipogenesis among male fetuses, which could manifest after adulthood, especially

upon high-fat insult. Our findings suggest that BPS exposure potentially exacerbates HFD-induced adipogenesis and presents a critical window of susceptibility by exposing pregnant mice to BPS for the second half of the gestation period. To our knowledge, our study is the first to reveal the male-specific adipogenic effects of mid-gestational exposure (9 d in utero) to BPS in F1 adults.

In the final study (Chapter 4), DNA methylation of adiposity-related imprinting gene in adipose tissue (especially eWAT) was evaluated to explain whether prenatal exposure to BPS affects fetal reprogramming. *Igf2/H19* was selected as the adiposity-related imprinting gene. We investigated effects of exposure on genomic imprinting in the mouse as imprinted genes are regulated by differential DNA methylation and aberrant imprinting disrupts fetal, placental, and postnatal development. The effect of BPS exposure during fetal development on the imprinting gene was investigated with DNA methylation of *Igf2/H19* ICR in gWAT. BPS-related CpG sites of *Igf2/H19* ICR were observed in gWAT. These results suggested that BPS exposure during mid-gestation can increase the levels of DNA methylation in *Igf2/H19* ICR and has an impact on specific CpG sites (GpG1 and CpG3) on it. We analyzed only six CpG sites within the target region for DNA methylation of *Igf2*. Despite screening of a limited number of CpG sites, our findings were meaningful and valuable in that we found BPS-responsive CpG sites of *Igf2/H19* ICR can exist.

In summary, the current research clearly demonstrated that (1) maternally exposure to BPS transferred to fetuses and retained in neonate, (2) prenatal BPS was related to the susceptibility to adiposity in adulthood and (3) altered the levels of DNA methylation in adiposity-related imprinting gene, *Igf2*, in white adipose tissues, and thus, (4) mid-gestation can be a sensitive window of fetal exposure to BPS.

Overall, this dissertation provides findings that have important implications for the understanding of the vulnerable period of BPS exposure to the adult-onset obesity. However, as most research, it suffers from a number of limitations.

First, there is a possibility that we could not catch remaining amount of BPS in lower exposure groups because of relatively higher detection limits. This limitation can be overcome by the technical development of analysis methods with significantly improved detection limits.

Second, while we observed BPS conjugate still retained in neonatal body of mice, a feasibility of extrapolation to human should be evaluated through further research considering inter-species differences in the metabolic clearance of BPS. The reason is because an *in vitro* study demonstrated that hepatic clearance of BPS in human was slower than in rodents although BPS is understood to be well absorbed and excreted mainly in urine with no species difference (Waidyanatha et

al. 2018).

Third, this study only involved male mice, based on previous studies on perinatal exposure to BPS and obesity having reported associations among male mice and sheep similar to human (Ivry Del Moral et al. 2016; Meng et al. 2018; Pu et al. 2017). Although a comparison was not made with female mice, it does not nullify the results obtained with male mice. Further studies are required to investigate sex-dependent adipogenic effects of BPS exposure.

Last, the experimental evidence of *Igf2* mRNA expression in placenta or gonadal white adipose tissue was ruled out. Future studies aiming at the identification of exact mechanistic link between DNA methylation of *Igf2* in gonadal white adipose tissue and mRNA expression in *Igf2*-expressed tissue would be critical. To overcome this limitations, clear consequences of BPS-induced epigenetic programming on adult-onset obesity remain to be elucidated in further investigations.

Overall, although several limitations exist, the findings of this dissertation have implications for human health by providing information on a critical window of exposure to BPS for adult-onset obesity management. It also provides fundamental data on BPS-specific CpGs of *Igf2*, especially considering that the imprinting regulation between mice and humans share similar features.

## **Bibliography**

Ahmed S, Atlas E. 2016. Bisphenol s- and bisphenol a-induced adipogenesis of murine preadipocytes occurs through direct peroxisome proliferator-activated receptor gamma activation. *International journal of obesity* 40:1566-1573.

Alonso-Magdalena P, Vieira E, Soriano S, Menes L, Burks D, Quesada I, et al. 2010. Bisphenol a exposure during pregnancy disrupts glucose homeostasis in mothers and adult male offspring. *Environmental health perspectives* 118:1243-1250.

Ariemma F, D'Esposito V, Liguoro D, Oriente F, Cabaro S, Liotti A, et al. 2016. Low-dose bisphenol-a impairs adipogenesis and generates dysfunctional 3t3-l1 adipocytes. *PLoS One* 11:e0150762.

Armitage JA, Poston L, Taylor PD. 2008. Developmental origins of obesity and the metabolic syndrome: The role of maternal obesity. *Frontiers of hormone research* 36:73-84.

Asimakopoulos AG, Xue J, De Carvalho BP, Iyer A, Abualnaja KO, Yaghmoor SS, et al. 2016. Urinary biomarkers of exposure to 57 xenobiotics and its association with oxidative stress in a population in jeddah, saudi arabia. *Environmental research* 150:573-581.

Baillie-Hamilton PF. 2002. Chemical toxins: A hypothesis to explain the global obesity epidemic. *J Altern Complement Med* 8:185-192.

Bansal A, Li C, Xin F, Duemler A, Li W, Rashid C, et al. 2019. Transgenerational

effects of maternal bisphenol: A exposure on offspring metabolic health. *Journal of developmental origins of health and disease* 10:164-175.

Barker DJ, Hales CN, Fall CH, Osmond C, Phipps K, Clark PM. 1993. Type 2 (non-insulin-dependent) diabetes mellitus, hypertension and hyperlipidaemia (syndrome x): Relation to reduced fetal growth. *Diabetologia* 36:62-67.

Barrett JR. 2017. Programming the future: Epigenetics in the context of dohad. *Environmental health perspectives* 125:A72.

Bastos Sales L, Kamstra JH, Cenijn PH, van Rijt LS, Hamers T, Legler J. 2013. Effects of endocrine disrupting chemicals on in vitro global DNA methylation and adipocyte differentiation. *Toxicology in vitro : an international journal published in association with BIBRA* 27:1634-1643.

Berni M, Gigante P, Bussolati S, Grasselli F, Grolli S, Ramoni R, et al. 2019. Bisphenol s, a bisphenol a alternative, impairs swine ovarian and adipose cell functions. *Domest Anim Endocrinol* 66:48-56.

Boucher JG, Ahmed S, Atlas E. 2016a. Bisphenol s induces adipogenesis in primary human preadipocytes from female donors. *Endocrinology* 157:1397-1407.

Boucher JG, Gagne R, Rowan-Carroll A, Boudreau A, Yauk CL, Atlas E. 2016b. Bisphenol a and bisphenol s induce distinct transcriptional profiles in differentiating human primary preadipocytes. *PLoS One* 11:e0163318.

Braun JM, Bellinger DC, Hauser R, Wright RO, Chen A, Calafat AM, et al. 2017. Prenatal phthalate, triclosan, and bisphenol a exposures and child visual-spatial

abilities. *Neurotoxicology* 58:75-83.

Breton CV, Marsit CJ, Faustman E, Nadeau K, Goodrich JM, Dolinoy DC, et al. 2017. Small-magnitude effect sizes in epigenetic end points are important in children's environmental health studies: The children's environmental health and disease prevention research center's epigenetics working group. *Environmental health perspectives* 125:511-526.

Callan AC, Hinwood AL, Heffernan A, Eaglesham G, Mueller J, Odland JO. 2013. Urinary bisphenol a concentrations in pregnant women. *Int J Hyg Environ Health* 216:641-644.

Chao HH, Zhang XF, Chen B, Pan B, Zhang LJ, Li L, et al. 2012. Bisphenol a exposure modifies methylation of imprinted genes in mouse oocytes via the estrogen receptor signaling pathway. *Histochem Cell Biol* 137:249-259.

Chen D, Kannan K, Tan H, Zheng Z, Feng YL, Wu Y, et al. 2016. Bisphenol analogues other than bpa: Environmental occurrence, human exposure, and toxicity-a review. *Environmental science & technology* 50:5438-5453.

Christensen KL, Lorber M, Koslitz S, Bruning T, Koch HM. 2012. The contribution of diet to total bisphenol a body burden in humans: Results of a 48 hour fasting study. *Environ Int* 50:7-14.

Chusyd DE, Wang D, Huffman DM, Nagy TR. 2016. Relationships between rodent white adipose fat pads and human white adipose fat depots. *Frontiers in nutrition* 3:10.

Constância M, Hemberger M, Hughes J, Dean W, Ferguson-Smith A, Fundele R, et al. 2002. Placental-specific igf-ii is a major modulator of placental and fetal growth. *Nature* 417:945-948.

Cooke PS, Naaz A. 2004. Role of estrogens in adipocyte development and function. *Exp Biol Med (Maywood)* 229:1127-1135.

Corbel T, Perdu E, Gayrard V, Puel S, Lacroix MZ, Viguié C, et al. 2015. Conjugation and deconjugation reactions within the fetoplacental compartment in a sheep model: A key factor determining bisphenol a fetal exposure. *Drug Metabolism and Disposition* 43:467-476.

da Silva BS, Pietrobon CB, Bertasso IM, Lopes BP, Carvalho JC, Peixoto-Silva N, et al. 2019. Short and long-term effects of bisphenol s (bps) exposure during pregnancy and lactation on plasma lipids, hormones, and behavior in rats. *Environ Pollut* 250:312-322.

Darbre PD. 2017. Endocrine disruptors and obesity. *Current obesity reports* 6:18-27.

Diamanti-Kandarakis E, Bourguignon JP, Giudice LC, Hauser R, Prins GS, Soto AM, et al. 2009. Endocrine-disrupting chemicals: An endocrine society scientific statement. *Endocr Rev* 30:293-342.

Donovan MJ, Paulino G, Raybould HE. 2009. Activation of hindbrain neurons in response to gastrointestinal lipid is attenuated by high fat, high energy diets in mice prone to diet-induced obesity. *Brain Res* 1248:136-140.



Doshi T, D'souza C, Vanage G. 2013. Aberrant DNA methylation at igf2-h19 imprinting control region in spermatozoa upon neonatal exposure to bisphenol a and its association with post implantation loss. *Molecular biology reports* 40:4747-4757.

Drobna Z, Henriksen AD, Wolstenholme JT, Montiel C, Lambeth PS, Shang S, et al. 2018. Transgenerational effects of bisphenol a on gene expression and DNA methylation of imprinted genes in brain. *Endocrinology* 159:132-144.

ECHA. 2014. 4,4'-sulphonyldiphenol [ec number: 201-250-5] repeated dose toxicity: Oral.

Eckardt M, Simat TJ. 2017. Bisphenol a and alternatives in thermal paper receipts - a german market analysis from 2015 to 2017. *Chemosphere* 186:1016-1025.

Egusquiza RJ, Blumberg B. 2020. Environmental obesogens and their impact on susceptibility to obesity: New mechanisms and chemicals. *Endocrinology* 161.

EU. 2011. European commission. Directive 2011/8/eu restricting the use of bisphenol a in plastic infant feeding bottles – eur-lex. Fed Reg Article 18 of Regulation (EC) No 1935/2004.

Evans RM, Barish GD, Wang YX. 2004. Ppars and the complex journey to obesity. *Nat Med* 10:355-361.

Even PC, Nadkarni NA. 2012. Indirect calorimetry in laboratory mice and rats: Principles, practical considerations, interpretation and perspectives. *American journal of physiology Regulatory, integrative and comparative physiology*

303:R459-476.

Fang C, Ning B, Waqar AB, Niimi M, Li S, Satoh K, et al. 2015. Bisphenol a exposure induces metabolic disorders and enhances atherosclerosis in hyperlipidemic rabbits. *Journal of applied toxicology* : JAT 35:1058-1070.

Faulk C, Dolinoy DC. 2011. Timing is everything: The when and how of environmentally induced changes in the epigenome of animals. *Epigenetics* 6:791-797.

Garcia-Arevalo M, Alonso-Magdalena P, Rebelo Dos Santos J, Quesada I, Carneiro EM, Nadal A. 2014. Exposure to bisphenol-a during pregnancy partially mimics the effects of a high-fat diet altering glucose homeostasis and gene expression in adult male mice. *PLoS One* 9:e100214.

Gauderat G, Picard-Hagen N, Toutain P-L, Corbel T, Viguié C, Puel S, et al. 2016. Bisphenol a glucuronide deconjugation is a determining factor of fetal exposure to bisphenol a. *Environment International* 86:52-59.

Gingrich J, Pu Y, Roberts J, Karthikraj R, Kannan K, Ehrhardt R, et al. 2018. Gestational bisphenol s impairs placental endocrine function and the fusogenic trophoblast signaling pathway. *Archives of toxicology* 92:1861-1876.

Gluckman PD, Hanson MA, Buklijas T, Low FM, Beedle AS. 2009. Epigenetic mechanisms that underpin metabolic and cardiovascular diseases. *Nature reviews Endocrinology* 5:401-408.

Grandin F, Picard-Hagen N, Gayrard V, Puel S, Viguie C, Toutain PL, et al. 2017.

Development of an on-line solid phase extraction ultra-high-performance liquid chromatography technique coupled to tandem mass spectrometry for quantification of bisphenol s and bisphenol s glucuronide: Applicability to toxicokinetic investigations. *J Chromatogr A* 1526:39-46.

Grandin FC, Lacroix MZ, Gayrard V, Gauderat G, Mila H, Toutain PL, et al. 2018. Bisphenol s instead of bisphenol a: Toxicokinetic investigations in the ovine materno-feto-placental unit. *Environ Int* 120:584-592.

Gregoire FM, Smas CM, Sul HS. 1998. Understanding adipocyte differentiation. *Physiological reviews* 78:783-809.

Grun F, Blumberg B. 2006. Environmental obesogens: Organotins and endocrine disruption via nuclear receptor signaling. *Endocrinology* 147:S50-55.

Grun F, Blumberg B. 2009. Endocrine disruptors as obesogens. *Mol Cell Endocrinol* 304:19-29.

Hehn RS. 2016. Nhanes data support link between handling of thermal paper receipts and increased urinary bisphenol a excretion. *Environ Sci Technol* 50:397-404.

Heindel JJ, Newbold R, Schug TT. 2015. Endocrine disruptors and obesity. *Nature reviews Endocrinology* 11:653-661.

Helies-Toussaint C, Peyre L, Costanzo C, Chagnon MC, Rahmani R. 2014. Is bisphenol s a safe substitute for bisphenol a in terms of metabolic function? An in vitro study. *Toxicol Appl Pharmacol* 280:224-235.

- Hines CJ, Jackson MV, Deddens JA, Clark JC, Ye X, Christianson AL, et al. 2017. Urinary bisphenol a (bpa) concentrations among workers in industries that manufacture and use bpa in the USA. *Ann Work Expo Health* 61:164-182.
- Huang RC, Galati JC, Burrows S, Beilin LJ, Li X, Pennell CE, et al. 2012. DNA methylation of the igf2/h19 imprinting control region and adiposity distribution in young adults. *Clinical epigenetics* 4:21.
- Ivry Del Moral L, Le Corre L, Poirier H, Niot I, Truntzer T, Merlin JF, et al. 2016. Obesogen effects after perinatal exposure of 4,4'-sulfonyldiphenol (bisphenol s) in c57bl/6 mice. *Toxicology* 357-358:11-20.
- Janesick A, Blumberg B. 2011. Endocrine disrupting chemicals and the developmental programming of adipogenesis and obesity. *Birth Defects Res C Embryo Today* 93:34-50.
- Kang ER, Iqbal K, Tran DA, Rivas GE, Singh P, Pfeifer GP, et al. 2011. Effects of endocrine disruptors on imprinted gene expression in the mouse embryo. *Epigenetics* 6:937-950.
- Kawamoto Y, Matsuyama W, Morikawa M, Morita M, Sugimoto M, Manabe N, et al. 2005. Disposition of bisphenol a in pregnant mice and fetuses after a single and repeated oral administration. *Toxicological & Environmental Chemistry* 87:199-213.
- Lakind JS, Naiman DQ. 2008. Bisphenol a (bpa) daily intakes in the united states: Estimates from the 2003-2004 nhanes urinary bpa data. *J Expo Sci Environ*

Epidemiol 18:608-615.

Lane RH. 2014. Fetal programming, epigenetics, and adult onset disease. Clinics in perinatology 41:815-831.

Le Fol V, Ait-Aissa S, Cabaton N, Dolo L, Grimaldi M, Balaguer P, et al. 2015. Cell-specific biotransformation of benzophenone-2 and bisphenol-s in zebrafish and human in vitro models used for toxicity and estrogenicity screening. Environ Sci Technol 49:3860-3868.

Lee J, Choi K, Park J, Moon HB, Choi G, Lee JJ, et al. 2018. Bisphenol a distribution in serum, urine, placenta, breast milk, and umbilical cord serum in a birth panel of mother-neonate pairs. Sci Total Environ 626:1494-1501.

Lee S, Kim C, Youn H, Choi K. 2017. Thyroid hormone disrupting potentials of bisphenol a and its analogues - in vitro comparison study employing rat pituitary (gh3) and thyroid follicular (ftrl-5) cells. Toxicology in vitro : an international journal published in association with BIBRA 40:297-304.

Lehmleer HJ, Liu B, Gadogbe M, Bao W. 2018. Exposure to bisphenol a, bisphenol f, and bisphenol s in u.S. Adults and children: The national health and nutrition examination survey 2013-2014. ACS omega 3:6523-6532.

Li Y, Perera L, Coons LA, Burns KA, Tyler Ramsey J, Pelch KE, et al. 2018. Differential in vitro biological action, coregulator interactions, and molecular dynamic analysis of bisphenol a (bpa), bpaf, and bps ligand-eralpha complexes. Environmental health perspectives 126:017012.

- Liao C, Liu F, Alomirah H, Loi VD, Mohd MA, Moon HB, et al. 2012. Bisphenol s in urine from the united states and seven asian countries: Occurrence and human exposures. *Environmental science & technology* 46:6860-6866.
- Liao C, Kannan K. 2013. Concentrations and profiles of bisphenol a and other bisphenol analogues in foodstuffs from the united states and their implications for human exposure. *J Agric Food Chem* 61:4655-4662.
- Liao C, Kannan K. 2014. A survey of bisphenol a and other bisphenol analogues in foodstuffs from nine cities in china. *Food additives & contaminants Part A, Chemistry, analysis, control, exposure & risk assessment* 31:319-329.
- Lin X, Lim IY, Wu Y, Teh AL, Chen L, Aris IM, et al. 2017. Developmental pathways to adiposity begin before birth and are influenced by genotype, prenatal environment and epigenome. *BMC medicine* 15:50.
- Liu B, Lehmler HJ, Sun Y, Xu G, Liu Y, Zong G, et al. 2017. Bisphenol a substitutes and obesity in us adults: Analysis of a population-based, cross-sectional study. *The Lancet Planetary health* 1:e114-e122.
- Liu B, Lehmler HJ, Sun Y, Xu G, Sun Q, Snetselaar LG, et al. 2019. Association of bisphenol a and its substitutes, bisphenol f and bisphenol s, with obesity in united states children and adolescents. *Diabetes & metabolism journal* 43:59-75.
- Liu J, Li J, Wu Y, Zhao Y, Luo F, Li S, et al. 2017. Bisphenol a metabolites and bisphenol s in paired maternal and cord serum. *Environmental science & technology* 51:2456-2463.

- Liu J, Wattar N, Field CJ, Dinu I, Dewey D, Martin JW, et al. 2018. Exposure and dietary sources of bisphenol a (bpa) and bpa-alternatives among mothers in the apron cohort study. *Environ Int* 119:319-326.
- Lorber M, Schechter A, Paepke O, Shropshire W, Christensen K, Birnbaum L. 2015. Exposure assessment of adult intake of bisphenol a (bpa) with emphasis on canned food dietary exposures. *Environ Int* 77:55-62.
- Manikkam M, Tracey R, Guerrero-Bosagna C, Skinner MK. 2013. Plastics derived endocrine disruptors (bpa, dehp and dbp) induce epigenetic transgenerational inheritance of obesity, reproductive disease and sperm epimutations. *PLoS One* 8:e55387.
- Martin EM, Fry RC. 2018. Environmental influences on the epigenome: Exposure-associated DNA methylation in human populations. *Annu Rev Public Health* 39:309-333.
- Matsumoto A, Kunugita N, Kitagawa K, Isse T, Oyama T, Foureman GL, et al. 2003. Bisphenol a levels in human urine. *Environ Health Perspect* 111:101-104.
- Mendonca K, Hauser R, Calafat AM, Arbuckle TE, Duty SM. 2014. Bisphenol a concentrations in maternal breast milk and infant urine. *Int Arch Occup Environ Health* 87:13-20.
- Meng Z, Wang D, Yan S, Li R, Yan J, Teng M, et al. 2018. Effects of perinatal exposure to bpa and its alternatives (bps, bpf and bpaf) on hepatic lipid and glucose homeostasis in female mice adolescent offspring. *Chemosphere* 212:297-306.

- Meng Z, Wang D, Liu W, Li R, Yan S, Jia M, et al. 2019. Perinatal exposure to bisphenol s (bps) promotes obesity development by interfering with lipid and glucose metabolism in male mouse offspring. *Environmental research* 173:189-198.
- Ng HW, Shu M, Luo H, Ye H, Ge W, Perkins R, et al. 2015. Estrogenic activity data extraction and in silico prediction show the endocrine disruption potential of bisphenol a replacement compounds. *Chemical research in toxicology* 28:1784-1795.
- Oh J, Choi JW, Ahn YA, Kim S. 2018. Pharmacokinetics of bisphenol s in humans after single oral administration. *Environ Int* 112:127-133.
- Ost A, Pospisilik JA. 2015. Epigenetic modulation of metabolic decisions. *Current opinion in cell biology* 33:88-94.
- Perera F, Herbstman J. 2011. Prenatal environmental exposures, epigenetics, and disease. *Reprod Toxicol* 31:363-373.
- Podrini C, Cambridge EL, Lelliott CJ, Carragher DM, Estabel J, Gerdin AK, et al. 2013. High-fat feeding rapidly induces obesity and lipid derangements in c57bl/6n mice. *Mammalian genome : official journal of the International Mammalian Genome Society* 24:240-251.
- Porras SP, Heinala M, Santonen T. 2014. Bisphenol a exposure via thermal paper receipts. *Toxicol Lett* 230:413-420.
- Pu Y, Gingrich JD, Steibel JP, Veiga-Lopez A. 2017. Sex-specific modulation of fetal adipogenesis by gestational bisphenol a and bisphenol s exposure.



Endocrinology 158:3844-3858.

Pu Y, Veiga-Lopez A. 2017. Pparggamma agonist through the terminal differentiation phase is essential for adipogenic differentiation of fetal ovine preadipocytes. Cellular & molecular biology letters 22:6.

Regnier SM, Sargis RM. 2014. Adipocytes under assault: Environmental disruption of adipose physiology. Biochim Biophys Acta 1842:520-533.

Reik W. 2007. Stability and flexibility of epigenetic gene regulation in mammalian development. Nature 447:425-432.

Rochester JR, Bolden AL. 2015. Bisphenol s and f: A systematic review and comparison of the hormonal activity of bisphenol a substitutes. Environ Health Perspect 123:643-650.

Rosen ED, Sarraf P, Troy AE, Bradwin G, Moore K, Milstone DS, et al. 1999. Ppar gamma is required for the differentiation of adipose tissue in vivo and in vitro. Mol Cell 4:611-617.

Saffery R, Novakovic B. 2014. Epigenetics as the mediator of fetal programming of adult onset disease: What is the evidence? Acta obstetricia et gynecologica Scandinavica 93:1090-1098.

Saigusa D, Okamura Y, Motoike IN, Katoh Y, Kurosawa Y, Saijyo R, et al. 2016. Establishment of protocols for global metabolomics by lc-ms for biomarker discovery. PLoS One 11:e0160555.

Sasaki H, Ishihara K, Kato R. 2000. Mechanisms of igf2/h19 imprinting: DNA

methylation, chromatin and long-distance gene regulation. *Journal of biochemistry* 127:711-715.

Schug TT, Janesick A, Blumberg B, Heindel JJ. 2011. Endocrine disrupting chemicals and disease susceptibility. *J Steroid Biochem Mol Biol* 127:204-215.

Shim WS, Do MY, Kim SK, Kim HJ, Hur KY, Kang ES, et al. 2006. The long-term effects of rosiglitazone on serum lipid concentrations and body weight. *Clin Endocrinol (Oxf)* 65:453-459.

Sidhu S, Parikh T, Burman KD. 2000. Endocrine changes in obesity. In: *Endotext*, (Feingold KR, Anawalt B, Boyce A, Chrousos G, Dungan K, Grossman A, et al., eds). South Dartmouth (MA).

Silva JPA, Ramos JG, Campos MS, da Silva Lima D, de Azevedo Brito PV, Mendes EP, et al. 2019. Bisphenol-s promotes endocrine-disrupting effects similar to those promoted by bisphenol-a in the prostate of adult gerbils. *Reproductive toxicology* 85:83-92.

Skledar DG, Schmidt J, Fic A, Klopčič I, Trontelj J, Dolenc MS, et al. 2016. Influence of metabolism on endocrine activities of bisphenol s. *Chemosphere* 157:152-159.

Smith CC, Taylor HS. 2007. Xenoestrogen exposure imprints expression of genes (*hoxa10*) required for normal uterine development. *FASEB J* 21:239-246.

Somm E, Schwitzgebel VM, Toulotte A, Cederroth CR, Combescure C, Nef S, et al. 2009. Perinatal exposure to bisphenol a alters early adipogenesis in the rat.

Environmental health perspectives 117:1549-1555.

Stel J, Legler J. 2015. The role of epigenetics in the latent effects of early life exposure to obesogenic endocrine disrupting chemicals. *Endocrinology* 156:3466-3472.

Susiarjo M, Sasson I, Mesaros C, Bartolomei MS. 2013. Bisphenol a exposure disrupts genomic imprinting in the mouse. *PLoS genetics* 9:e1003401.

Thayer KA, Taylor KW, Garantziotis S, Schurman SH, Kissling GE, Hunt D, et al. 2016. Bisphenol a, bisphenol s, and 4-hydroxyphenyl 4-isopropoxyphenylsulfone (bpsip) in urine and blood of cashiers. *Environmental health perspectives* 124:437-444.

Tudurí E, Marroqui L, Dos Santos RS, Quesada I, Fuentes E, Alonso-Magdalena P. 2018. Timing of exposure and bisphenol-a: Implications for diabetes development. *Frontiers in Endocrinology* 9.

U.S.EPA. 1988. Bisphenol a.

USFDA. 2012. Final rule. Indirect food additives: Polymers [docket no. Fda-2012-f-0031]. *Fed Reg* FDA-2012-F-0031.

USFDA. 2013. Final rule. Indirect food additives: Adhesives and components of coatings [docket no. Fda-2012-f-0728].

Vandenberg LN, Ehrlich S, Belcher SM, Ben-Jonathan N, Dolinoy DC, Hugo ER, et al. 2013. Low dose effects of bisphenol a. *Endocrine Disruptors* 1:e26490.

Veiga-Lopez A, Pu Y, Gingrich J, Padmanabhan V. 2018. Obesogenic endocrine

disrupting chemicals: Identifying knowledge gaps. Trends in endocrinology and metabolism: TEM 29:607-625.

Vervliet P, Gys C, Caballero-Casero N, Covaci A. 2019. Current-use of developers in thermal paper from 14 countries using liquid chromatography coupled to quadrupole time-of-flight mass spectrometry. Toxicology 416:54-61.

Vinas R, Watson CS. 2013. Bisphenol s disrupts estradiol-induced nongenomic signaling in a rat pituitary cell line: Effects on cell functions. Environmental health perspectives 121:352-358.

Vom Saal FS, Nagel SC, Coe BL, Angle BM, Taylor JA. 2012. The estrogenic endocrine disrupting chemical bisphenol a (bpa) and obesity. Mol Cell Endocrinol 354:74-84.

Waidyanatha S, Black SR, Snyder RW, Yueh YL, Sutherland V, Patel PR, et al. 2018. Disposition and metabolism of the bisphenol analogue, bisphenol s, in harlan sprague dawley rats and b6c3f1/n mice and in vitro in hepatocytes from rats, mice, and humans. Toxicol Appl Pharmacol 351:32-45.

Wan Y, Huo W, Xu S, Zheng T, Zhang B, Li Y, et al. 2018. Relationship between maternal exposure to bisphenol s and pregnancy duration. Environ Pollut 238:717-724.

Want EJ, Masson P, Michopoulos F, Wilson ID, Theodoridis G, Plumb RS, et al. 2013. Global metabolic profiling of animal and human tissues via uplc-ms. Nat Protoc 8:17-32.

Wassenaar PNH, Trasande L, Legler J. 2017. Systematic review and meta-analysis of early-life exposure to bisphenol a and obesity-related outcomes in rodents. *Environmental health perspectives* 125:106001.

Wei J, Lin Y, Li Y, Ying C, Chen J, Song L, et al. 2011. Perinatal exposure to bisphenol a at reference dose predisposes offspring to metabolic syndrome in adult rats on a high-fat diet. *Endocrinology* 152:3049-3061.

WHO. 2018. Fact sheet on obesity and overweight. World health organization. Available: <https://www.who.int/en/news-room/fact-sheets/detail/obesity-and-overweight> [accessed 16 February 2018].

WHO/FAO. 2011. Toxicological and health aspects of bisphenol a. (Joint FAO/WHO expert meeting to review toxicological and health aspects of bisphenol A: final report, including report of stakeholder meeting on bisphenol A, 1-5 November 2010, Ottawa, Canada). ISBN 978 92 14 156427 4. World Health Organization.

WHO/UNEP. 2013. State of the science of endocrine disrupting chemicals - 2012: An assessment of the state of the science of endocrine disruptors prepared by a group of experts for the united nations environment programme (unep) and who. Geneva:WHO.

Yamada L, Chong S. 2017. Epigenetic studies in developmental origins of health and disease: Pitfalls and key considerations for study design and interpretation. *Journal of developmental origins of health and disease* 8:30-43.

- Yan Z, Liu Y, Yan K, Wu S, Han Z, Guo R, et al. 2017. Bisphenol analogues in surface water and sediment from the shallow chinese freshwater lakes: Occurrence, distribution, source apportionment, and ecological and human health risk. *Chemosphere* 184:318-328.
- Ye X, Wong LY, Kramer J, Zhou X, Jia T, Calafat AM. 2015. Urinary concentrations of bisphenol a and three other bisphenols in convenience samples of u.S. Adults during 2000-2014. *Environmental science & technology* 49:11834-11839.
- Zhang T, Sun H, Kannan K. 2013. Blood and urinary bisphenol a concentrations in children, adults, and pregnant women from china: Partitioning between blood and urine and maternal and fetal cord blood. *Environ Sci Technol* 47:4686-4694.
- Zhang X, Ji M, Tan X, Yu K, Xu L, Chen G, et al. 2019. Role of epigenetic regulation of igf2 and h19 in 2,3,7,8-tetrachlorobenzo-p-dioxin (tcdd)-induced ovarian toxicity in offspring rats. *Toxicology letters* 311:98-104.
- Zhang XF, Zhang LJ, Feng YN, Chen B, Feng YM, Liang GJ, et al. 2012. Bisphenol a exposure modifies DNA methylation of imprint genes in mouse fetal germ cells. *Molecular biology reports* 39:8621-8628.
- Zhang YF, Ren XM, Li YY, Yao XF, Li CH, Qin ZF, et al. 2018. Bisphenol a alternatives bisphenol s and bisphenol f interfere with thyroid hormone signaling pathway in vitro and in vivo. *Environ Pollut* 237:1072-1079.
- Zhou X, Kramer JP, Calafat AM, Ye X. 2014. Automated on-line column-switching high performance liquid chromatography isotope dilution tandem mass

spectrometry method for the quantification of bisphenol a, bisphenol f, bisphenol s, and 11 other phenols in urine. *J Chromatogr B Analyt Technol Biomed Life Sci* 944:152-156.

Zhu Z, Cao F, Li X. 2019. Epigenetic programming and fetal metabolic programming. *Front Endocrinol (Lausanne)* 10:764.

## 국 문 초 록 (Abstract in Korean)

### 비스페놀 S 의 산전 노출과 비만 감수성의 변화

서울대학교 보건대학원

환경보건학 전공

안 영 아

비스페놀 S (BPS)는 비스페놀 A (BPA)의 독성과 건강 유해성을 이유로 전세계적으로 사용이 금지되자 대체제로 등장하였다. 현재 BPS는 다양한 나라에서 실내 공기와 생체시료에서 검출되고 있다. 특히, 산모의 생체 시료 중 BPS 검출은 태반을 통한 태아의 노출 가능성까지 제기되어 생애초기 노출의 건강영향이 우려되고 있다. 내분비계장애물질 (Endocrine Disrupting Chemical; EDC)로 알려진 BPA는 태중 노출 시 태아 발달뿐만 아니라, 청소년기와 성인기의 비만을 비롯한 대사성 질환에 영향을 줄 수 있다고 보고된다. 전문가들은 BPA와 구조적으로 유사한 BPS도 BPA와 유사한 건강영향을 미칠 수 있다고 보고하고 있다. 최근 태아 발달시기를



포함한 생애초기 노출과 건강영향에 관한 연구가 증가하고 있으나, 여전히 산전 BPS 노출과 성체 지방 생성에 관한 연구는 부족하다.

생애초기 노출 연구가 중요한 이유는 태중 (*in utero*)과 영유아기는 체내 기관 형성 및 발달 시기로 그 기능이 미숙하여 노출물질의 대사와 체외 배출이 어려워질 수 있기 때문이다. 또한, 생애초기 환경이 이후 건강과 질병의 기원이 될 수 있음을 의미하는 DOHaD (Developmental Origins of Health and Disease) 가설을 기반으로 한 많은 연구들이 생애초기 다양한 EDCs 물질이 비만유발환경물질 (Obesogens)으로 작용하여 성인기 비만을 일으킬 수 있다고 보고하고 있다. 이러한 맥락에서 생애초기 환경과 출생 이후 건강영향을 잘 이해하기 위해서는 후성유전적 접근을 필요로 한다. 그러나 현재 BPS 산전노출에 따른 비만 영향 연구에 후성유전학적 연구는 제한적이며, 동물 실험을 통한 생애초기 노출과 후성유전적 변화에 관한 연구는 매우 부족하다.

본 연구의 최종 목표는 BPS 산전 노출로 인한 성체기 비만 감수성을 변화를 설명하는 것이다. 이를 위해, 임신마우스를 이용하여 BPS 노출 모델을 구축하였으며, 임신 9일차부터 임신 18일차 (출산 직전)까지 식수를 통한 BPS 경구 노출을 수행하였다. 먼저 모체를 통한 후속세대 F1의 BPS 노출 여부와 관련 대사체를 파악하고 (Chapter 2), BPS 산전노출에 의한

성체기의 비만 표현형 변화와 지방생성 관련 유전자의 발현량 변화를 통해 드러난 비만 감수성의 변화를 설명하며 (Chapter 3), 마지막으로 각인유전자 *Igf2*의 DNA 메틸화 변화 여부를 살펴보았다 (Chapter 4).

첫 번째 연구 (Chapter 2)에서는 모체를 통한 BPS 노출이 태아에 전달될 수 있는지를 비롯하여 노출이 중단된 출생 이후 체외 배출이 용이한 대사체 (예. BPS-G, BPS-S)를 생성하는지 살펴보기 위해 수행되었다. 임신마우스를 통해 임신 9일차부터 출산직전까지 다양한 용량의 BPS (0, 0.05, 0.5, 5, 50 mg/kg/d)를 식수를 통해 지속적으로 노출시켰다. 후속 세대 출생 직후 (PND 1)의 간(liver)과 간을 제외한 전신(whole body without liver)을 수집하여 UPLC-qTOF-MS로 BPS와 그 대사체를 측정하고 정량하였다. 분석 결과는 어미에게 노출시킨 BPS는 태아에게 전달되었음을 나타내었다. 검출수준 한계로 BPS 50 mg/kg/d 그룹의 생체시료에서만 정량 가능하였다. 성체의 주요 대사체로 알려진 BPS-G로 알려진 것과 달리, 본 연구에서는 PND1 (생후 1일차)에서 높은 검출률을 보이는 대사체는 BPS-S으로 나타났다. 또한 BPS 노출 중단 이후 1일째 되었을 때 어미로부터 전달된 BPS의 14.6%가 체내 남아있었다. 이 연구의 결과는 성체기 대사 특성과 달리 출생직후에는 체외 배출이 쉬운 대사체로 알려

진 BPS-G보다 상당량의 free-BPS가 존재하고 BPS-S의 형태로 대사되고 있음을 실험적으로 확인한 사례로써 중요한 의의를 지닌다.

두 번째 연구 (Chapter 3)에서는 BPS 산전 노출이 성체기 지방 생성에 영향을 줄 수 있는지 살펴보기 위한 목적으로 수행되었다. 모체를 통한 BPS 노출은 출생 이후에 이루어지지 않았으며, 성체기 (8-10주령)가 되었을 때 비만 표현형인 체중, 생식기 주변의 백색지방 (gWAT) 무게, 지방세포의 크기와 수를 관찰하여 BPS 노출 그룹간 비교하였다. 비만 감수성 변화를 뚜렷하게 관찰하기 위해 지방조직 발달이 끝나는 6주령부터 단기간 (4주)의 고지방식이 (HFD)를 추가하였다. 또한 지방생성과 관련 유전자 (adipogenic marker genes) 변화를 살펴보기 위해 모든 노출 그룹의 gWAT에서 *Pparg*, *Cebp  $\alpha$* , *Fabp4*, *Lpl*, *Adipoq*의 mRNA 발현량을 비교하였다. 이 연구에서는 BPS에 산전 노출된 후 HFD가 수행된 수컷에서 체중 대비 gWAT 무게 비율의 증가를 확인하였으며, 본 연구의 모든 BPS 노출용량 그룹에서 gWAT 지방세포 수와 크기의 유의한 증가가 있었다. 그리고 BPS 5 mg/kg/d와 50 mg/kg/d 그룹에서 HFD 수컷의 지방생성 관련 유전자 mRNA 발현량의 유의미한 증가가 있었다. 특히 표준식이 (STD) 그룹의 *Lpl* mRNA 발현량 증가는 지방생성 표현형이 드러나지 않아도 지

지방 생성 감수성 변화가 있음을 잘 보여준다. 본 연구를 통해 BPS 산전노출이 지방 생성 기전에 관여할 수 있음을 유전자 발현량 차이를 통해 실험적으로 증명하였다. 관찰된 지방생성 관련 유전자가 5개라는 점은 본 연구의 한계점으로 보일 수 있으나, BPS 산전노출 그룹 간 지방생성 유전자 발현량의 뚜렷한 차이는 BPS 노출 특이적 지방 생성 기전이 있음을 의미한다.

세 번째 연구 (Chapter 4)에서는 BPS 산전노출로 인한 후성유전학적 변화를 비만 관련 각인유전자 *Igf2/H19 ICR*의 DNA 메틸화를 통해 설명하고자 하였다. gWAT 으로부터 genomic DNA를 추출하고 Bisulfite 처리를 거쳐 Pyrosequencing을 수행함으로써 *Igf2/H19 ICR*에서의 DNA 메틸화 비율을 측정하였다. BPS 산전노출량에 따른 메틸화를 전체적으로 비교하고, 선정된 6개 CpG site 중 BPS에 영향을 받은 CpC site를 탐색하였다. 각 CpG sites 별 BPS 산전노출에 의한 DNA 메틸화 차이는 비모수 검정(Kruskal-Wallis)을 수행하여 나타냈다. 선정된 6개의 CpG sites 전체의 DNA 메틸화는 평균 50% 이하였으며, BPS 산전노출 그룹 간 DNA 메틸화의 통계적 차이를 보이지 않았다 ( $p>0.05$ ). 한편, *Igf2* CpG site 별로 DNA 메틸화를 살펴본 결과, BPS 산전노출 이후 STD 그룹에서는 CpG5와 CpG6에서의 DNA 메틸화 수준의 노출 그룹 간 유의미한 차이를 보였으

며, BPS 산전노출 HFD 그룹의 CpG1과 CpG3에서 DNA 메틸화의 유의한 차이를 나타내었다. BPS 생애초기 노출 이후 STD를 유지할 경우 비만 표현형을 관찰할 수 없었지만, 특정 CpG sites에서 *Igf2*의 DNA 메틸화 변화를 보인 것으로 보아 BPS 산전 노출이 임신 중기부터 수행되어도 후성유전학적 변화에 영향을 미칠 수 있다는 것을 증명했다. 각인유전자 *Igf2*의 모든 CpG sites를 스크리닝하지 않았기 때문에 전체 메틸화 변화를 나타낼 수 없다는 한계점이 있음에도 불구하고, 본 연구는 BPA의 *Igf2/H19* DMR 변화를 보인 선행연구와 달리, BPS 산전노출 시 *Igf2/H19* ICR의 DNA 메틸화 증가가 나타날 수 있음을 보여주기 때문에 BPS 특이적 후성유전적 기전이 있을 수 있음을 시사하고 있다. 또한 특정 BPS-responsive CpG site를 제시함으로써, 후속연구의 후성유전적 기전 이해에 도움을 줄 수 있는 연구로도 가치가 있다.

종합적으로 BPS 산전 노출로 인한 성체기 지방생성과 후성유전적 영향에 관한 세 연구를 통해, (1) 어미를 통한 BPS 노출이 태아 및 신생 마우스에도 전달될 수 있음을 확인하였으며, (2) BPS 산전노출이 성체기 지방생성 감수성에 영향을 줄 수 있음을 증명하였으며, (3) gWAT에서 비만 관련 각인유전자 *Igf2*의 DNA 메틸화 증가를 통해 임신중기의 BPS 노출이

후성유전적 변화에 영향을 줄 수 있음을 보여줌으로써 최종 연구 목표를 달성하였다. 보건학적으로 중요한 비만을 다양한 DOHaD 연구 사례와 같이 성인 생애초기 환경 노출로부터 접근할 수 있었다. 특히 본 연구의 특징점은 BPS의 중요한 노출 시기를 동물실험을 통해 증명했다는 점과 임신 중기에서 출산직전까지 짧은 기간의 BPS 노출만으로도 비만감수성에 영향을 줄 수 있음을 보여주었다는 것에 있다. 다만 비만 감수성 변화에 어떤 후성유전적 기전이 어떻게 관여하는지에 대한 생물학적 이해를 위해 후속 연구가 필요할 것으로 생각된다.

**Keywords:** 비스페놀 S, 산전노출, 지방생성, 지방생성 마커 유전자, 각인유전자, DNA 메틸화

**Student Number: 2016-30659**